cardiovascular events (standard correlation coefficients [β] = 0.549, $P < 0.001$) and serum levels of hsTNF-α ($\beta = 0.235$, $P = 0.038$) were independently associated with AER. Age ($\beta = 0.398$, $P < 0.001$), SBP ($\beta = 0.227$, $P = 0.035$), duration of diabetes ($\beta = 0.210$, $P = 0.041$) and serum levels of IP-10 ($\beta = 0.209$, $P = 0.047$), were independently associated with baPWV. Serum levels of IP-10 ($\beta = 0.303$, $P = 0.032$) was independently associated with IMT.

4. Discussion

The current study has revealed that serum levels of various proinflammatory cytokines, chemokines and adhesion molecules associate with the severity of diabetic nephropathy and atherosclerosis. Proinflammatory molecules may compose a complex network in the kidney and atherosclerotic lesion and contribute to make pathologic lesions in diabetic patients. Our result suggests that serum levels of proinflammatory cytokines, chemokines and adhesion molecules may associate with the local change of these proinflammatory molecules in diabetic kidney and atherosclerotic lesion. Moreover, we have shown that TNF-α and IP-10 could be useful markers for the progression of diabetic nephropathy and atherosclerosis. Our data may provide important findings about the local inflammatory network in diabetic vascular complications.

Serum levels of several proinflammatory molecules were significantly increased in type 2 diabetic patients. Several reports also revealed that serum levels of these proinflammatory cytokines and chemokines were elevated in type 2 diabetic patients [19–21]. The simple correlation analysis in type 2 diabetic patients showed that both TNF-α and IP-10 significantly correlated with AER, baPWV and IMT. Moreover, in the multiple regression analysis, TNF-α was independently associated with AER and IP-10 was independently associated with baPWV and IMT. These results suggest that TNF-α strongly contributes to diabetic nephropathy and IP-10 strongly associates with atherosclerosis. Serum levels of TNF-α and VCAM-1 were not significantly higher in diabetic patients than in control subjects; however, these were correlated with AER and baPWV in type 2 diabetic patients. The age of control subjects was relatively high in our study. It might be one of the causes that the serum levels of TNF-α and VCAM-1 were similar between diabetic patients and control subjects [22].

In control subjects, simple correlation was found between serum levels of hsTNF-α and AER and between serum levels of ICAM-1 and baPWV or IMT. However, neither of these molecules was independently associated with AER, baPWV and IMT in multiple linear regression analysis (data not shown). Thus, our result might be characteristic changes in type 2 diabetic patients.

It is reported that vascular endothelial dysfunction due to oxidative stress was induced by increasing TNF-α in the coronary artery of Zucker obese fatty rats [23]. Over-expression of TNF-α was also observed in the glomeruli of streptozotocin-induced diabetic rats [24]. In another report, serum TNF-α was increased in diabetic patients with albuminuria as compared with patients without albuminuria [25]. These reports support our current finding and suggest that TNF-α contributes to glomerular injuries in diabetic patients.

IP-10 is a potent mitogenic and chemotaxic factor for vascular smooth muscle cells [4]. In the atheroma of human carotid artery, the expression of IP-10 and its receptor CXCR3 and increased invasion of T cells were observed [26]. IP-10 was also reported to participate in the formation of atherosclerotic lesions through mediating inflammatory cell invasion [4]. Taken together, elevated serum level of IP-10 may predict the increased production in atherosclerotic lesions in diabetic patients. With the view to the relationship between IP-10 and diabetic nephropathy, over-expression of IP-10 mRNA was observed in the tubulo-intestinal compartments of renal tissues from patients with diabetic nephropathy [27]. Increased IP-10 expression in the tubulo-interstitial cells was observed in the puromycin aminonucleoside (PAN) nephrosis of rats [28], which is the model of nephrotic syndrome and tubulo-intestinal nephritis. Moreover, human mesangial cells expressed CXCR3 and IP-10 stimulated proliferation of the cells [29]. These reports indicate that IP-10 might be involved in the pathogenesis of diabetic nephropathy as well as of atherosclerosis.

There was overlap in the serum levels of proinflammatory molecules and AER, baPWV and IMT between diabetic patients and control subjects in this study. There was a wide distribution of the severity of diabetic complications and atherosclerosis in diabetic participants. In addition, the sample size of our study was relatively small. Thus, this large overlap might be caused by small sample size and sample distribution. Relationships between serum proinflammatory cytokine concentrations and behavior of cytokines within target organs have remained unclear. It has also remained unclear why serum cytokines elevates in diabetic patients. Further long-term prospective study and *in vitro* analysis are required to clarify these mechanisms.

In conclusion, microinflammation may be a common risk factor for progression of atherosclerosis and diabetic nephropathy in patients with type 2 diabetes.

Conflict of interest

There are no conflicts of interest.

Acknowledgements

This study was supported in part by Grants-in-Aid for Scientific Research from the Ministry of Education, Science, Culture, Sports and Technology of Japan and Health Sciences Research Grants conducted by Ministry of Health Labor and Welfare. We thank colleagues on the medical staff at Okayama Saiseikai General Hospital who supported this study.

REFERENCES

[1] R. Ross, Atherosclerosis—an inflammatory disease, N. Engl. J. Med. 340 (1999) 115–126.

[2] J.K. Pai, T. Pischon, J. Ma, J.E. Manson, S.E. Hankinson, K. Joshipura, et al., Inflammatory markers and the risk of coronary heart disease in men and women, N. Engl. J. Med. 351 (2004) 2599–2610.
[3] J. de Jager, J.M. Dekker, A. Kooy, P.J. Kostense, G. Nijpels, R.J. Heine, et al., Endothelial dysfunction and low-grade inflammation explain much of the excess cardiovascular mortality in individuals with type 2 diabetes: the Hoorn study, Arterioscler. Thromb. Vasc. Biol. 26 (2006) 1086–1093.
[4] X. Wang, T.L. Yue, E.H. Ohlstein, C.P. Sung, G.Z. Feuerstein, Interferon-inducible protein-10 involves vascular smooth muscle cell migration, proliferation, and inflammatory response, J. Biol. Chem. 271 (1996) 24286–24293.
[5] A. Festa, R. D'Agostino, G. Howard, L. Mykkänen, R.P. Tracy, S.M. Haffner, Inflammation and microalbuminuria in nondiabetic and type 2 diabetic subjects: the insulin resistance atherosclerosis study, Kidney Int. 58 (2000) 1703–1710.
[6] J.C. Pickup, G.D. Chusney, S.M. Thomas, D. Burt, Plasma interleukin-6, tumour necrosis factor alpha and blood cytokine production in type 2 diabetes, Life Sci. 67 (2000) 291–300.
[7] A. Festa, R. D'Agostino Jr., G. Howard, L. Mykkänen, R.P. Tracy, S.M. Haffner, Chronic subclinical inflammation as part of the insulin resistance syndrome: the insulin resistance atherosclerosis study (IRAS), Circulation 102 (2000) 42–47.
[8] A.D. Pradhan, J.E. Manson, N. Rifai, J.E. Buring, P.M. Ridker, C-reactive protein, interleukin 6, and risk of developing type 2 diabetes mellitus, JAMA 286 (2001) 327–334.
[9] F. Arnalich, A. Hernanz, D. Lopez-Maderuelo, J.M. Pena, J. Camacho, R. Madero, et al., Enhanced acutephase response and oxidative stress in older adults with type II diabetes, Horm. Metab. Res. 32 (2000) 407–412.
[10] K. Esposito, F. Nappo, R. Marfella, G. Giugliano, F. Giugliano, M. Ciotola, et al., Inflammatory cytokine concentrations are acutely increased by hyperglycemia in humans: role of oxidative stress, Circulation 106 (2002) 2067–2072.
[11] K. Hirata, K. Shikata, M. Matsuda, K. Akiyama, H. Sugimoto, M. Kushiro, et al., Increased expression of selectins in kidneys of patients with diabetic nephropathy, Diabetologia 41 (1998) 185–192.
[12] H. Sugimoto, K. Shikata, K. Hirata, K. Akiyama, M. Matsuda, M. Kushiro, et al., Increased expression of intercellular adhesion molecule-1 (ICAM-1) in diabetic rat glomeruli: glomerular hyperfiltration is a potential mechanism of ICAM-1 upregulation, Diabetes 46 (1997) 2075–2081.
[13] J.P. Albertini, P. Valensi, B. Lormeau, M.H. Aurousseau, F. Ferrière, J.R. Attali, et al., Elevated concentrations of soluble E-selectin and vascular cell adhesion molecule-1 in NIDDM. Effect of intensive insulin treatment, Diabetes Care 21 (1998) 1008–1013.
[14] S. Okada, K. Shikata, M. Matsuda, D. Ogawa, H. Usui, Y. Kido, et al., Intercellular adhesion molecule-1-deficient mice are resistant against renal injury after induction of diabetes, Diabetes 52 (2003) 2586–2593.
[15] A. Nakamura, K. Shikata, M. Hiramatsu, T. Nakatou, T. Kitamura, J. Wada, et al., Serum interleukin-18 levels are associated with nephropathy and atherosclerosis in Japanese patients with type 2 diabetes, Diabetes Care 28 (2005) 2890–2985.
[16] G. Bruno, P. Cavallo-Perin, G. Bargero, M. Borra, N. D'Errico, G. Pagano, Association of fibrinogen with glycemic control and albumin excretion rate in patients with non-insulin-dependent diabetes mellitus, Ann. Intern. Med. 125 (1996) 653–657.
[17] L. Mykkanen, D. Zaccaro, D. O'Leary, G. Howard, D. Robbins, S. Haffner, Microalbuminuria and carotid artery intimamedia thickness in nondiabetic and NIDDM subjects: the insulin resistance atherosclerosis study (IRAS), Stroke 28 (1997) 1710–1716.
[18] H. Yokoyama, T. Aoki, M. Imahori, M. Kuramitsu, Subclinical atherosclerosis is increased in type 2 diabetic patients with microalbuminuria evaluated by intima-media thickness and pulse wave velocity, Kidney Int. 66 (2004) 448–454.
[19] J.F. Navarro, C. Mora, M. Gómez, M. Muros, C. López-Aguilar, J. García, Influence of renal involvement on peripheral blood mononuclear cell expression behaviour of tumour necrosis factor-alpha and interleukin-6 in type 2 diabetic patients, Nephrol. Dial. Transplant. 23 (2008) 919–926.
[20] S. Mine, Y. Okada, T. Tanikawa, C. Kawahara, T. Tabata, Y. Tanaka, Increased expression levels of monocyte CCR2 and monocyte chemoattractant protein-1 in patients with diabetes mellitus, Biochem. Biophys. Res. Commun. 344 (2006) 780–785.
[21] S. Kiyici, E. Erturk, F. Budak, C. Ersoy, E. Tuncel, C. Duran, et al., Serum monocyte chemoattractant protein-1 and monocyte adhesion molecules in type 1 diabetic patients with nephropathy, Arch. Med. Res. 37 (2006) 998–1003.
[22] L. O'Mahony, J. Holland, J. Jackson, C. Feighery, T.P. Hennessy, K. Mealy, Quantitative intracellular cytokine measurement: age-related changes in proinflammatory cytokine production, Clin. Exp. Immunol. 113 (1998) 213–219.
[23] A. Picchi, X. Gao, S. Belmadani, B.J. Potter, M. Focardi, W.M. Chilian, et al., Tumor necrosis factor-α induces endothelial dysfunction in the prediabetic metabolic syndrome, Circ. Res. 99 (2006) 69–77.
[24] H. Sugimoto, K. Shikata, J. Wada, S. Horiuchi, H. Makino, Advanced glycation end products-cytokine–nitric oxide sequence pathway in the development of diabetic nephropathy: aminoguanidine ameliorates the overexpression of tumour necrosis factor-alpha and inducible nitric oxide synthase in diabetic rat glomeruli, Diabetologia 42 (1999) 878–886.
[25] Y. Moriwaki, T. Yamamoto, Y. Shibutani, E. Aoki, Z. Tsutsumi, S. Takahashi, et al., Elevated levels of interleukin-18 and tumor necrosis factor-alpha in serum of patients with type 2 diabetes mellitus: relationship with diabetic nephropathy, Metabolism 52 (2003) 605–608.
[26] F. Mach, A. Sauty, A.S. Iarossi, G.K. Sukhova, K. Neote, P. Libby, et al., Differential expression of three T lymphocyte-activating CXC chemokines by human atheroma-associated cells, J. Clin. Invest. 104 (1999) 1041–1050.
[27] H. Schmid, A. Boucherot, Y. Yasuda, A. Henger, B. Brunner, F. Eichinger, et al., European Renal cDNA Bank (ERCB) Consortium. Modular activation of nuclear factor-kappaB transcriptional programs in human diabetic nephropathy, Diabetes 55 (2006) 2993–3003.
[28] W.W. Tang, M. Qi, J.S. Warren, G.Y. Van, Chemokine expression in experimental tubulointerstitial nephritis, J. Immunol. 159 (1997) 870–876.
[29] A. Bonacchi, P. Romagnani, R.G. Romanelli, E. Efsen, F. Annunziato, L. Lasagni, et al., Signal transduction by the chemokine receptor CXCR3: activation of Ras/ERK, Src, and phosphatidylinositol 3-kinase/Akt controls cell migration and proliferation in human vascular pericytes, J. Biol. Chem. 276 (2001) 9945–9954.

Hindawi Publishing Corporation
Experimental Diabetes Research
Volume 2011, Article ID 534872, 8 pages
doi:10.1155/2011/534872

Research Article

High Glucose Increases Metallothionein Expression in Renal Proximal Tubular Epithelial Cells

Daisuke Ogawa,[1,2] Masato Asanuma,[3] Ikuko Miyazaki,[3] Hiromi Tachibana,[1] Jun Wada,[1] Norio Sogawa,[4] Takeshi Sugaya,[5] Shinji Kitamura,[1] Yohei Maeshima,[1] Kenichi Shikata,[1,6] and Hirofumi Makino[1]

[1] *Department of Medicine and Clinical Science, Okayama University Graduate School of Medicine, Dentistry and Pharmaceutical Sciences, Okayama 700-8558, Japan*
[2] *Department of Diabetic Nephropathy, Okayama University Graduate School of Medicine, Dentistry and Pharmaceutical Sciences, Okayama 700-8558, Japan*
[3] *Department of Brain Science, Okayama University Graduate School of Medicine, Dentistry and Pharmaceutical Sciences, Okayama 700-8558, Japan*
[4] *Department of Dental Pharmacology, Okayama University Graduate School of Medicine, Dentistry and Pharmaceutical Sciences, Okayama 700-8558, Japan*
[5] *CMIC Company, Ltd., Tokyo 113-0034, Japan*
[6] *Center for Innovative Clinical Medicine, Okayama University Hospital, Okayama 700-8558, Japan*

Correspondence should be addressed to Daisuke Ogawa, daiogawa@md.okayama-u.ac.jp

Received 25 May 2011; Revised 25 July 2011; Accepted 31 July 2011

Academic Editor: Yasuhiko Tomino

Metallothionein (MT) is an intracellular metal-binding, cysteine-rich protein, and is a potent antioxidant that protects cells and tissues from oxidative stress. Although the major isoforms MT-1 and -2 (MT-1/-2) are highly inducible in many tissues, the distribution and role of MT-1/-2 in diabetic nephropathy are poorly understood. In this study, diabetes was induced in adult male rats by streptozotocin, and renal tissues were stained with antibodies for MT-1/-2. MT-1/-2 expression was also evaluated in mProx24 cells, a mouse renal proximal tubular epithelial cell line, stimulated with high glucose medium and pretreated with the antioxidant vitamin E. MT-1/-2 expression was gradually and dramatically increased, mainly in the proximal tubular epithelial cells and to a lesser extent in the podocytes in diabetic rats, but was hardly observed in control rats. MT-1/-2 expression was also increased by high glucose stimulation in mProx24 cells. Because the induction of MT was suppressed by pretreatment with vitamin E, the expression of MT-1/-2 is induced, at least in part, by high glucose-induced oxidative stress. These observations suggest that MT-1/-2 is induced in renal proximal tubular epithelial cells as an antioxidant to protect the kidney from oxidative stress, and may offer a novel therapeutic target against diabetic nephropathy.

1. Introduction

Diabetic nephropathy is a leading cause of end-stage renal disease, and many mechanisms have been proposed to explain the pathogenesis of renal injury in diabetes [1]. Recent studies have shown that hyperglycemia may induce oxidative stress by increasing reactive oxygen species (ROS) generation in the diabetic kidney [2–4] and that overexpression of the antioxidant superoxide dismutase 1 attenuated diabetic nephropathy in streptozotocin (STZ)-induced and *db*/*db* diabetic mice [5, 6]. Therefore, ROS could be an important mediator of diabetic nephropathy, and protection from ROS might offer a valuable therapeutic strategy to treat diabetic nephropathy.

Metallothionein (MT) is an intracellular metal-binding protein with a low-molecular mass (6-7 kDa) and a high cysteine content (20 of 61-62 amino acids). Its major isoforms, MT-1 and -2 (MT-1/-2), are widely distributed

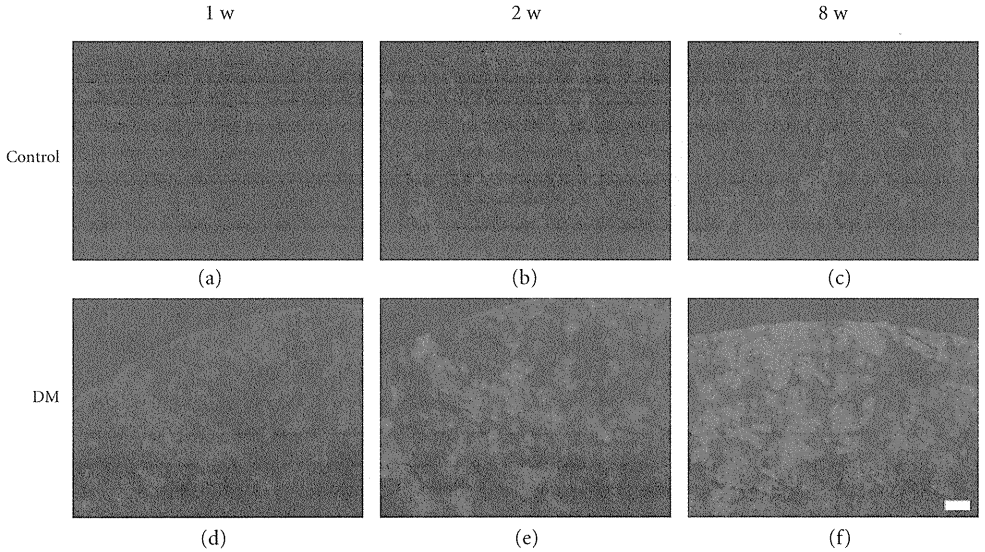

FIGURE 1: MT-1/-2 expression in the kidney. Diabetes was induced by injection of streptozotocin, and kidneys were obtained at 1 (a and d), 2 (b and e), or 8 (c and f) weeks after inducing diabetes. Immunofluorescent staining was performed as described in *Materials and Methods*. MT was strongly expressed in the renal cortex of diabetic rats (d, e, f) and hardly expressed in control rats (a, b, c). The expression of MT-1/-2 was greater at week 8 than at weeks 1 and 2 after diabetes induction. Scale bar: 100 μm.

throughout the body [7, 8]. Since MT-1/-2 expression is significantly upregulated by overload of essential trace metals (e.g., Zn and Cu), it plays an important role in heavy metal detoxification and essential metal homeostasis [9, 10]. In addition, MTs have been shown to act as nonspecific free radical scavengers [11, 12], suggesting that they exert antioxidant activities in various diseases, including diabetic nephropathy.

We and other investigators have demonstrated that MTs have neuroprotective effects in mouse models of Parkinson's disease [13–15]. In contrast, the role of MTs in the pathogenesis of diabetic nephropathy is poorly understood. Several studies reported that renal expression of MT is increased in STZ-induced diabetic rats [16], diabetic BB rats [17], and *ob/ob* diabetic mice [18]. However, the distribution of MTs in the diabetic kidney and the mechanisms by which MTs are induced in diabetes are poorly understood. Therefore, in the present study, we investigated the expression and localization of MT-1/-2 during the development of diabetic nephropathy and explored the mechanism by which MT-1/-2 expression was induced by high glucose in the kidney.

2. Materials and Methods

2.1. Experimental Protocol. Male Sprague Dawley rats were purchased from Charles River (Yokohama, Japan). Five-week-old rats were divided into two groups: (1) nondiabetic control rats (control; $n = 6$) and (2) STZ-induced diabetic rats (DM; $n = 6$). Diabetes was induced by peritoneal injection of 200 mg/kg STZ (Sigma-Aldrich Corp., MO) in citrate buffer (pH 4.5). Blood glucose was measured by the glucose oxidase method at 3 days after STZ injection and only rats with blood glucose concentrations >16 mmol/L were used in the study. All rats had free access to standard diet and tap water. All procedures were performed according to the Guidelines for Animal Experiments at Okayama University Medical School, Japanese Government Animal Protection and Management Law (No. 105) and the Japanese Government Notification on Feeding and Safekeeping of Animals (No. 6). Rats were sacrificed at 1, 2, or 8 weeks after inducing diabetes. We measured body weight, hemoglobin A1c (HbA1c), and 24-h urinary albumin excretion (UAE) at 1, 2, and 8 weeks. The kidneys were removed, weighed, and fixed in 10% formalin for periodic acid—methenamine silver (PAM) staining, and parts of the remaining tissues were embedded in optimal cutting temperature compound (Sakura Finetechnical, Tokyo, Japan) and frozen immediately in acetone cooled on dry ice.

2.2. Immunofluorescent Staining of MT-1/-2 in Rat Kidney. Immunofluorescent staining was performed as previously described [19]. Renal expression of MT-1/-2 was detected using mouse anti-MT-1/-2 antibody (Dako, Carpinteria, CA) followed by Alexa Fluor 594 goat anti-mouse IgG (Invitrogen, Carlsbad, CA). To determine whether MT-1/-2 was localized in podocytes or proximal tubular epithelial cells, the sections were counterstained with guinea pig antinephrin antibody (Fitzgerald, Concord, MA) or rabbit antiaquaporin 1 antibody (Millipore, Billerica, MA), followed by Alexa Fluor 488 goat anti-guinea pig IgG or anti-rabbit IgG (Invitrogen), respectively. Fluorescence images were obtained using a fluorescence microscope (BX51; Olympus, Tokyo, Japan).

2.3. Cell Culture and Treatment. mProx24 cells, a murine renal proximal tubular epithelial cell line derived from

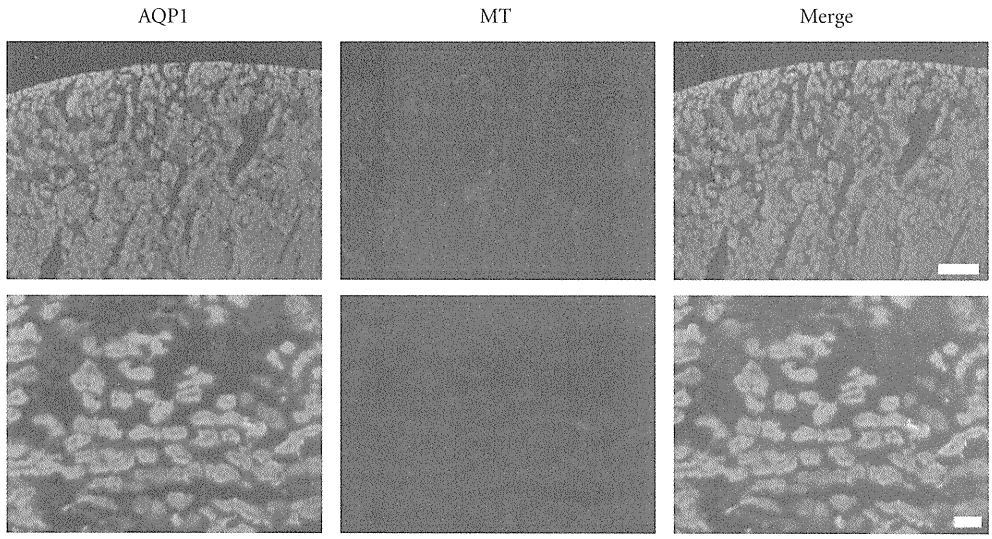

(a)

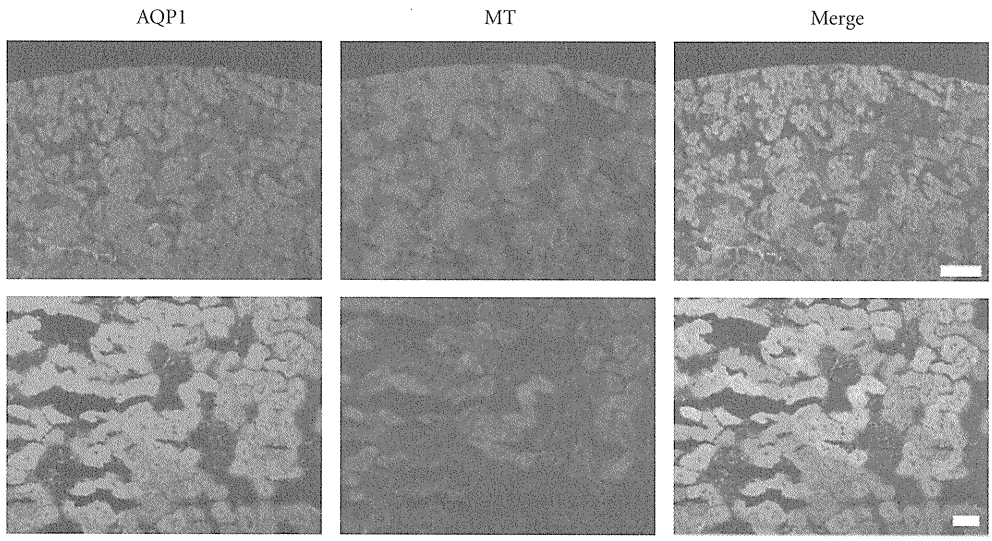

(b)

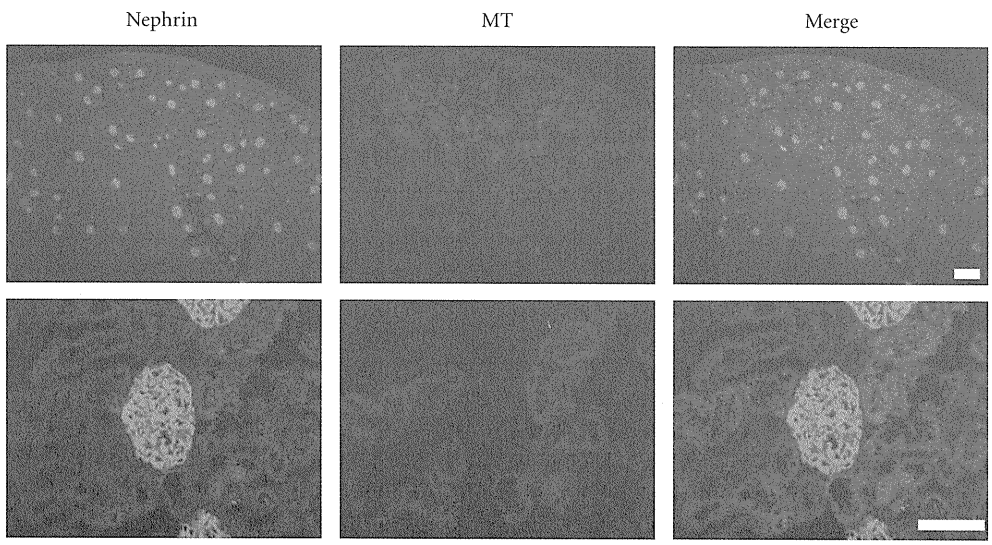

(c)

FIGURE 2: Continued.

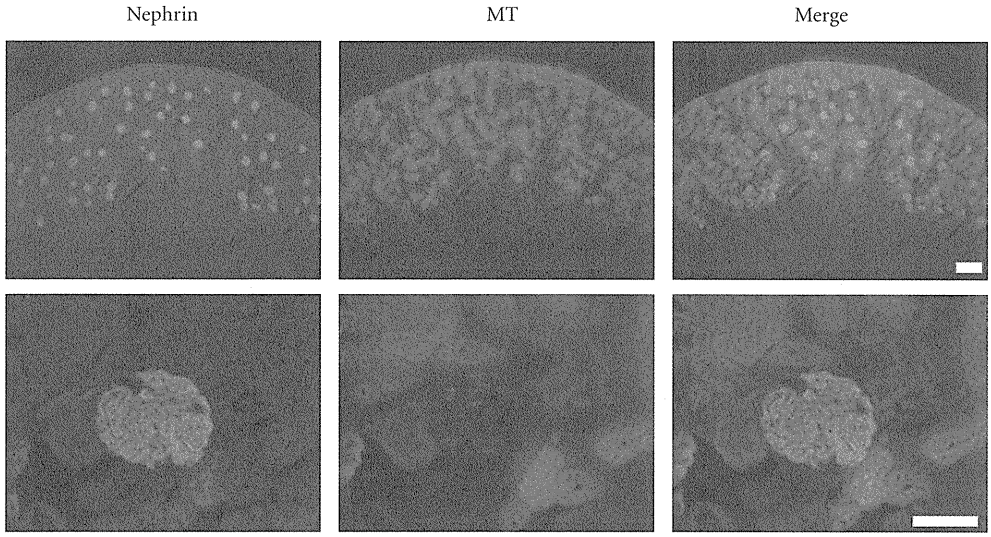

(d)

FIGURE 2: MT-1/-2 expression in podocytes and proximal tubular cells of the kidney. Immunofluorescent staining was performed as described in *Materials and Methods*. Eight weeks after inducing diabetes, MT-1/-2 was predominantly expressed in the proximal tubular epithelial cells of the kidney (b) and weakly expressed in podocytes (d) in the kidney of diabetic rats. In control rats, MT-1/-2 was weakly expressed in proximal tubular epithelial cells (a), but hardly in the podocytes (c). AQP1: aquaporin 1, MT: MT-1/-2. Scale bar: upper panels, 200 μm; lower panels, 50 μm.

C57BL/6J adult mouse kidney [20], were cultured in Dulbecco's modified Eagle's medium (Sigma-Aldrich Corp.) supplemented with 1000 mg/L D-glucose, 10% fetal bovine serum, 100 U/mL penicillin, and 100 mg/mL streptomycin at 37°C in 5% CO_2. To evaluate the effect of high glucose on MT expression, the cells were serum-starved by culture in 0.5% FBS for 24 h, then stimulated with 4500 mg/L D-glucose (high glucose) or D-mannitol (Sigma-Aldrich Corp.) for 24 h. For antioxidant treatment, the cells were pretreated with vitamin E (Sigma-Aldrich Corp.) at concentration ranges from 20 to 200 nM for 24 h, then stimulated with high glucose for 24 h. Individual experiments were repeated at least three times with different lots or preparations of cells.

2.4. Quantitative Analyses of MT-1 Gene and MT-1/-2 Protein Expression in mProx Cells. RNA was isolated from mProx cells using an RNeasy Mini kit (Qiagen, Valencia, CA). Single-strand cDNA was synthesized from the extracted RNA using a RT-PCR kit (Perkin Elmer, Foster City, CA). To evaluate the mRNA expression of MT-1 in mProx24 cells, quantitative RT-PCR (qRT-PCR) was performed using StepOnePlus (Applied Biosystems, Tokyo, Japan) and Fast-Start SYBR Premix Ex Taq II (Takara Bio Inc., Otsu, Japan). The primers for the MT-1 gene (upstream 5′-TCTAAGCGTCACCACGACTTCA-3′ and downstream 5′-GTGCACTTGCAGTTCTTGCAG-3′) were purchased from Takara Bio Inc. Each sample was analyzed in triplicate and normalized for GAPDH mRNA expression. Immunofluorescent staining of MT-1/-2 protein was performed as described above. The immunofluorescence intensity in cultured mProx cells was calculated using the formula, x (density) × positive area (μm^2), using Lumina Vision software (Mitani Corporation).

2.5. Statistical Analysis. All values are means ± SEM. Statistically significant differences between groups were examined using one-way ANOVA followed by Scheffé's test. Values of $P < 0.05$ were considered statistically significant.

3. Results

3.1. MT-1/-2 Expression Was Increased in Diabetic Kidney. MT-1/-2 expression was observed in the renal cortex from 1 week after the induction of diabetes. Its expression increased gradually and was strongly upregulated at week 8 (Figure 1,(d),(e),(f)). In contrast, MT-1/-2 was hardly detected in the kidney of control rats (Figure 1, (a),(b),(c)). Renal sections counterstained with antiaquaporin 1 and antinephrin antibodies revealed that MT-1/-2 expression was predominantly localized in the proximal tubular epithelial cells (Figure 2(b)), and to a lesser extent in the podocytes of the diabetic kidneys (Figure 2(d)). In control rats, MT-1/-2 was weakly expressed in the proximal tubular epithelial cells (Figure 2(a)), but not in the podocytes (Figure 2(c)). Body weight, kidney weight, UAE, and HbA1c are shown in Table 1. Diabetic rats had a significantly lower body weight and higher kidney weight per body weight at 8 weeks, but not at 1 and 2 weeks after the induction of diabetes. Similarly, The UAE and HbA1c level in the diabetic rats was significantly higher than in the control rats at 8 weeks, but not at 1 and 2 weeks. Glomerular hypertrophy and mesangial matrix expansion, but not interstitial changes and tubular atrophy

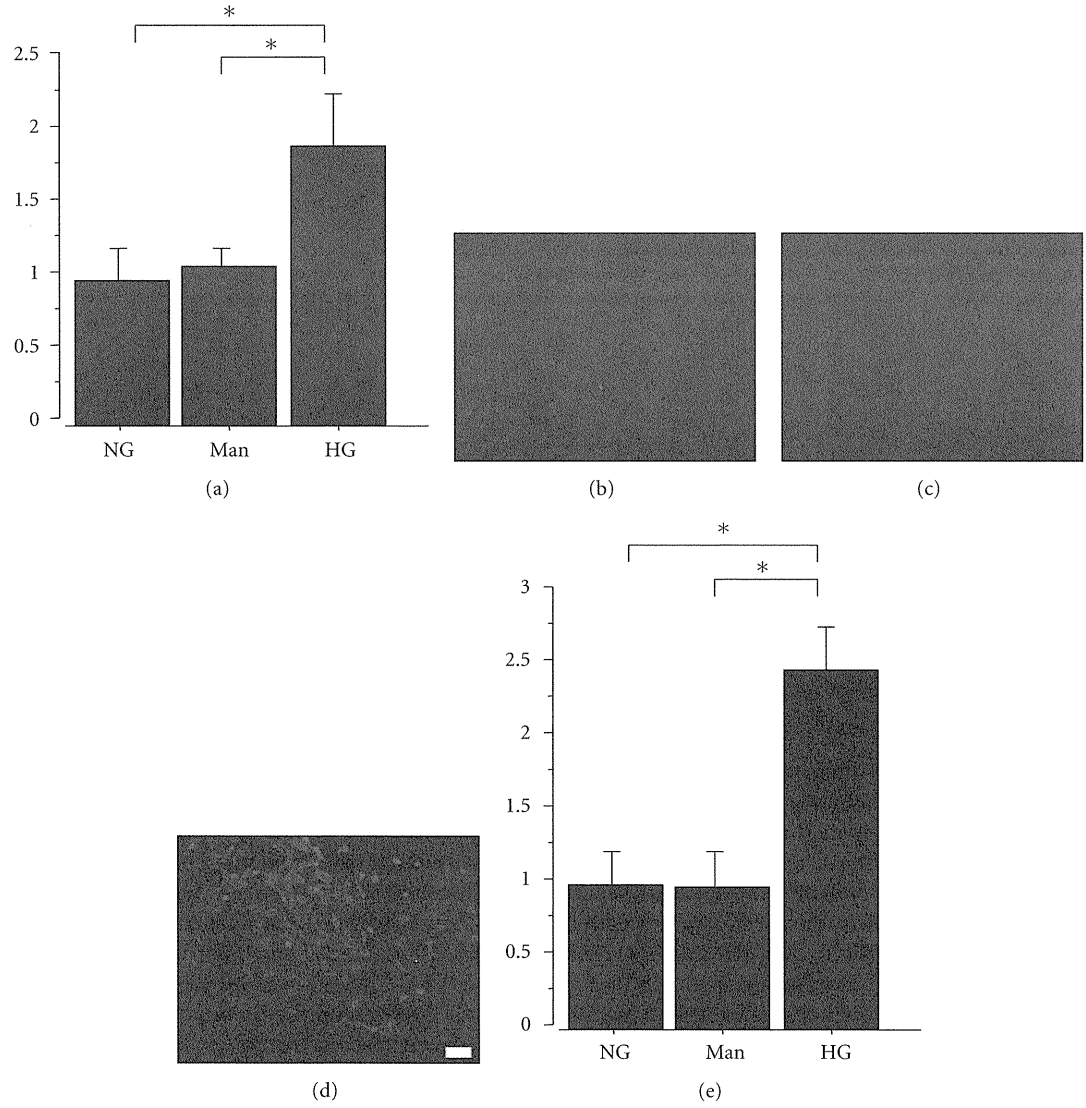

FIGURE 3: High glucose increases MT-1 mRNA and MT-1/-2 protein expression. mProx24 cells were serum-starved for 24 h before stimulation with high glucose or mannitol. (a) Cells were harvested after 24 h, and MT-1 mRNA expression was analyzed by qRT-PCR in three independent experiments and normalized for GAPDH. (b–e) MT-1/-2 protein expression was determined by immunofluorescent staining with anti-MT-1/-2 antibody 24 h after stimulation followed by densitometric analysis. Results are means ± SEM of three independent experiments. $^*P < 0.05$ versus high glucose; NG: normal glucose; Man: mannitol; HG: high glucose. Scale bar: 100 μm.

were observed in the diabetic rats as compared with control rats at 8 weeks (data not shown).

3.2. High Glucose Increased MT-1/-2 Expression in mProx24 Cells. qRT-PCR analyses revealed that exposure to the high glucose medium significantly increased MT-1 mRNA expression in mProx24 cells compared with normal glucose medium (Figure 3(a)). Similarly, high glucose, but not mannitol, significantly increased MT-1/-2 protein expression in mProx24 cells (Figures 3(b)–3(e)). These data indicate that high glucose increases the mRNA and protein expression of MT-1/-2 in mProx24 cells.

3.3. MT-1/-2 Expression Was Suppressed by Vitamin E. It is well known that high glucose increases the generation of ROS in various cells. To investigate the mechanism by which MT is induced by ROS in the high glucose condition, we examined the effects of an antioxidant, vitamin E, on MT-1/-2 expression in mProx24 cells. As shown in Figure 4, high-glucose-stimulated MT-1/-2 expression was significantly attenuated by vitamin E in a dose-dependent manner (Figure 4). Accordingly, these findings suggest that ROS generated by high glucose induces MT-1/-2 expression in the proximal tubular epithelial cells of the kidney.

4. Discussion

There is increasing evidence from experimental and clinical studies to suggest that oxidative stress plays a critical role in the pathogenesis and progression of diabetic

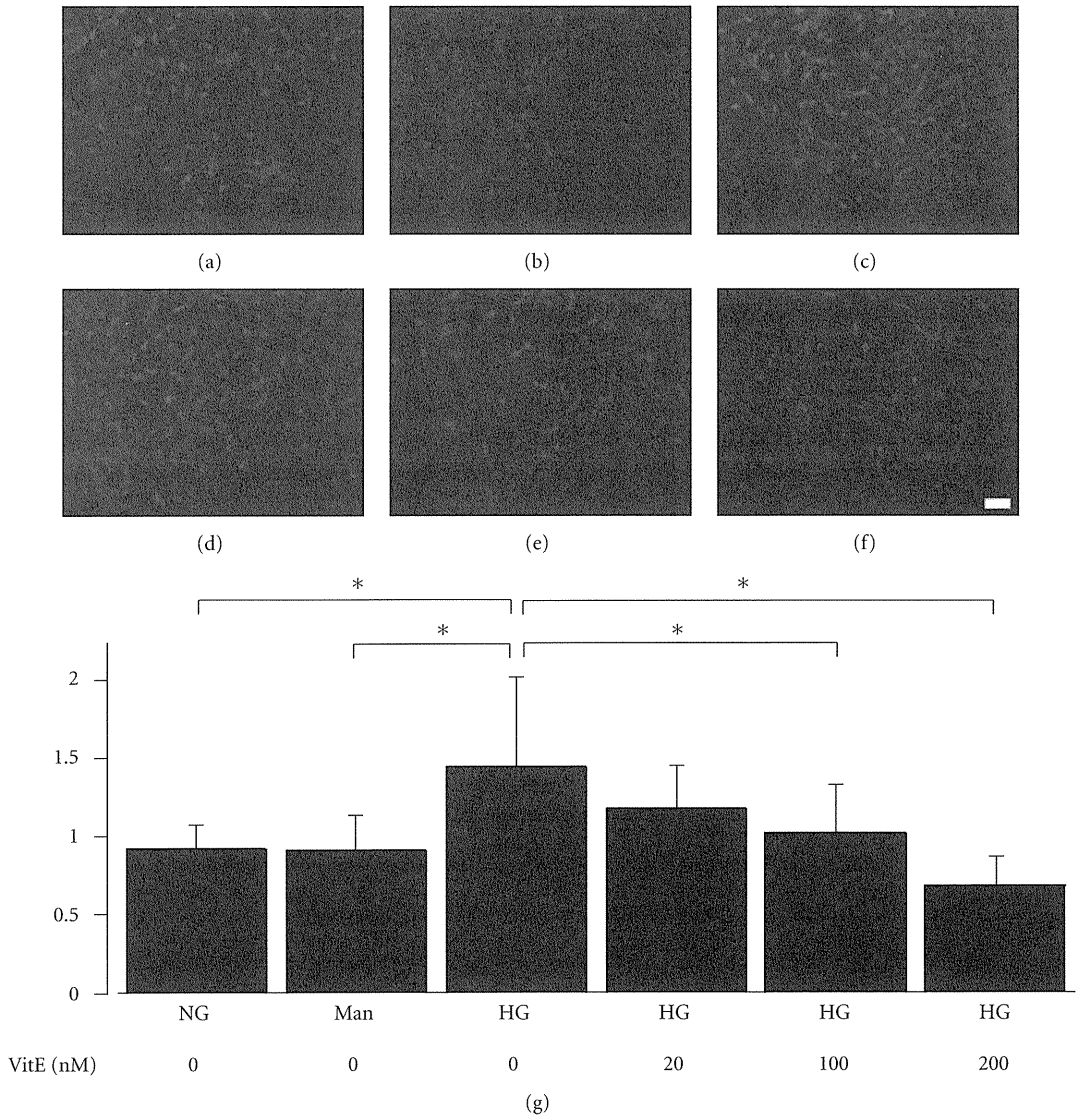

FIGURE 4: Vitamin E suppresses high glucose-induced MT-1/-2 expression. mProx24 cells were serum-starved and pretreated with vehicle or vitamin E for 24 h before stimulation with high glucose or mannitol. MT-1/-2 expression was determined by immunofluorescent staining. MT-1/-2 expression was not increased by mannitol (b) compared with normal glucose (a), but was increased by high glucose (c). High glucose-induced MT-1/-2 expression was attenuated by vitamin E pretreatment in a dose-dependent manner (d: 20 nM; E: 100 nM; F: 200 nM). The cells depicted are representative of three independent experiments. (g) Densitometric quantification of MT-1/-2 immunofluorescence. Results are means ± SEM of three independent experiments. $^*P < 0.05$ versus high glucose; NG: normal glucose; Man: mannitol; HG: high glucose; Vit E: vitamin E. Scale bar: 100 μm.

complications [21]. Since MT is a potent, endogenous and inducible antioxidant in various tissues [11, 12], we hypothesized that MT may be induced and act as an antioxidant in STZ-induced diabetic kidneys. Here, we found that high glucose induces the expression of MT-1/-2 mainly in proximal tubular epithelial cells and, to a lesser extent, in podocytes in rat kidneys. MT-1/-2 was dramatically expressed in renal proximal tubular epithelial cells within 1 week after inducing diabetes and gradually increased to week 8. MT-1/-2 expression seems to correlate with glucose level, but not with UAE, HbA1c, interstitial abnormalities. To our knowledge, this is the first report describing the localization and expression of MT-1/-2 in the diabetic kidney.

To elucidate the mechanism by which diabetes induces MT-1/-2 expression in proximal tubular epithelial cells, we investigated the effects of high glucose stimulation on mProx24, a murine renal proximal tubular epithelial cell line. We detected increased MT-1 mRNA and MT-1/-2 protein expression in the high glucose condition and found that high glucose-induced MT-1/-2 expression was suppressed by pretreatment with the antioxidant vitamin E. Vitamin E is well known to have high biological activity to protect cells from the propagation of free radical reactions [22, 23], thus we chose vitamin E in this study. These data suggest that ROS and oxidative stress, which are induced by high glucose, may be involved in the induction of MT-1/-2. Although

Table 1: Metabolic data at 1, 2, and 8 weeks after inducing diabetes.

	1 week	2 week	8 week
Body weight (g)			
Control	204 ± 6.3	241 ± 10.4	380 ± 13.3
Diabetic	198 ± 4.7	225 ± 11.5	248 ± 16.6*
Kidney weight (mg/g BW)			
Control	5.8 ± 0.4	5.6 ± 0.8	4.5 ± 0.7
Diabetic	5.9 ± 0.6	6.1 ± 1.0	6.7 ± 0.9*
UAE (μg/day)			
Control	110 ± 7.3	121 ± 8.1	137 ± 14.7
Diabetic	116 ± 5.7	125 ± 9.4	458 ± 24.5*
HbA1c (%)			
Control	3.7 ± 0.4	3.8 ± 0.6	3.8 ± 0.5
Diabetic	3.8 ± 0.3	4.3 ± 0.7	7.8 ± 0.9*

Data are means ± SEM; *$P < 0.05$ versus the control group. BW: body weight; UAE: urinary albumin excretion; HbA1c: hemoglobin A1c.

several studies have shown that MT protein expression is increased in the kidney of diabetic animals [16–18], the cellular distribution of MTs has not been addressed. Our data provide the first evidence for the expression profile of MT-1/-2 in the diabetic kidney. We speculate that MT-1/-2 is highly induced in proximal tubular epithelial cells in compensation for oxidative stress induced by high glucose.

Our study has potential limitations. First, we speculated that MT-1/-2 expression was upregulated by ROS, but further studies are needed to elucidate the underlying mechanisms. Although Zn is known to induce the gene and protein expression of MTs [24], this essential trace element is unlikely to be involved in our findings because the same chow was provided to the control and diabetic rats. In this study, we showed that high-glucose-stimulated MT-1/-2 expression was attenuated by vitamin E *in vitro*, but we have no data about diabetic rats treated by vitamin E. MT-1/-2 expression in the diabetic state may differ between cells and tissues, and the mechanisms by which other antioxidants regulate the expression of MT remain unclear. Further studies are needed to elucidate these issues. Second, it is still controversial whether site-specific induction of MT plays an important role in diabetic nephropathy. Podocyte-specific overexpression of MT reduced diabetic nephropathy in transgenic mice [25]. However, no studies have investigated whether MT expression in proximal tubular epithelial cells has a protective effect in diabetic animal models. Therefore, diabetes models using MT-knockout mice are needed to answer this question.

In conclusion, renal ROS, which are induced by diabetes, upregulate MT-1/-2 expression in proximal tubular epithelial cells of the kidney. Our results suggest that MT-1/-2 might be a novel therapeutic target to treat diabetic nephropathy.

Acknowledgments

This study was supported in part by a Grant-in-Aid for Young Scientists (B) from the Ministry of Education, Culture, Sports, Science and Technology, Japan, to Dr. Ogawa (21790813) and by a Grant-in-Aid for Diabetic Nephropathy from the Ministry of Health, Labour and Welfare of Japan. This work has received support from the Takeda Science Foundation and the Naito Foundation. The authors have no potential conflicts of interests relevant to this study to report.

References

[1] A. E. Declèves and K. Sharma, "New pharmacological treatments for improving renal outcomes in diabetes," *Nature Reviews Nephrology*, vol. 6, no. 6, pp. 371–380, 2010.

[2] J. W. Baynes and S. R. Thorpe, "Role of oxidative stress in diabetic complications: a new perspective on an old paradigm," *Diabetes*, vol. 48, no. 1, pp. 1–9, 1999.

[3] T. Nishikawa, D. Edelstein, X. L. Du et al., "Normalizing mitochondrial superoxide production blocks three pathways of hyperglycaemic damage," *Nature*, vol. 404, no. 6779, pp. 787–790, 2000.

[4] T. Matsuoka, J. Wada, I. Hashimoto et al., "Gene delivery of Tim44 reduces mitochondrial superoxide production and ameliorates neointimal proliferation of injured carotid artery in diabetic rats," *Diabetes*, vol. 54, no. 10, pp. 2882–2890, 2005.

[5] P. A. Craven, M. F. Melhem, S. L. Phillips, and F. R. DeRubertis, "Overexpression of Cu^{2+}/Zn^{2+} superoxide dismutase protects against early diabetic glomerular injury in transgenic mice," *Diabetes*, vol. 50, no. 9, pp. 2114–2125, 2001.

[6] F. R. DeRubertis, P. A. Craven, M. F. Melhem, and E. M. Salah, "Attenuation of renal injury in db/db mice overexpressing superoxide dismutase: evidence for reduced superoxide-nitric oxide interaction," *Diabetes*, vol. 53, no. 3, pp. 762–768, 2004.

[7] D. H. Hamer, "Metallothionein," *Annual Review of Biochemistry*, vol. 55, pp. 913–951, 1986.

[8] M. Vasak, "Advances in metallothionein structure and functions," *Journal of Trace Elements in Medicine and Biology*, vol. 19, no. 1, pp. 13–17, 2005.

[9] P. J. Thornalley and M. Vasak, "Possible role for metallothionein in protection against radiation-induced oxidative stress. Kinetics and mechanism of its reaction with superoxide and hydroxyl radicals," *Biochimica et Biophysica Acta*, vol. 827, no. 1, pp. 36–44, 1985.

[10] R. D. Palmiter, "The elusive function of metallothioneins," *Proceedings of the National Academy of Sciences of the United States of America*, vol. 95, no. 15, pp. 8428–8430, 1998.

[11] Y. J. Kang, Y. Chen, A. Yu, M. Voss-McCowan, and P. N. Epstein, "Overexpression of metallothionein in the heart of transgenic mice suppresses doxorubicin cardiotoxicity," *Journal of Clinical Investigation*, vol. 100, no. 6, pp. 1501–1506, 1997.

[12] A. R. Quesada, R. W. Byrnes, S. O. Krezoski, and D. H. Petering, "Direct reaction of H_2O_2 with sulfhydryl groups in HL-60 cells: zinc- metallothionein and other sites," *Archives of Biochemistry and Biophysics*, vol. 334, no. 2, pp. 241–250, 1996.

[13] M. Ebadi, H. Brown-Borg, H. El Refaey et al., "Metallothionein-mediated neuroprotection in genetically engineered mouse models of Parkinson's disease," *Molecular Brain Research*, vol. 134, no. 1, pp. 67–75, 2005.

[14] I. Miyazaki, M. Asanuma, H. Hozumi, K. Miyoshi, and N. Sogawa, "Protective effects of metallothionein against dopamine quinone-induced dopaminergic neurotoxicity," *FEBS Letters*, vol. 581, no. 25, pp. 5003–5008, 2007.

[15] I. Miyazaki, M. Asanuma, Y. Kikkawa et al., "Astrocyte-derived metallothionein protects dopaminergic neurons from

dopamine quinone toxicity," *Glia*, vol. 59, no. 3, pp. 435–451, 2011.

[16] M. L. Failla and R. A. Kiser, "Altered tissue content and cytosol distribution of trace metals in experimental diabetes," *Journal of Nutrition*, vol. 111, no. 11, pp. 1900–1909, 1981.

[17] M. L. Failla and C. Y. Gardell, "Influence of spontaneous diabetes on tissue status of zinc, copper, and manganese in BB Wistar rat," *Proceedings of the Society for Experimental Biology and Medicine*, vol. 180, no. 2, pp. 317–322, 1985.

[18] M. L. Kennedy and M. L. Failla, "Zinc metabolism in genetically obese (ob/ob) mice," *Journal of Nutrition*, vol. 117, no. 5, pp. 886–893, 1987.

[19] S. Okada, K. Shikata, M. Matsuda et al., "Intercellular adhesion molecule-1-deficient mice are resistant against renal injury after induction of diabetes," *Diabetes*, vol. 52, no. 10, pp. 2586–2593, 2003.

[20] S. Kitamura, Y. Maeshima, T. Sugaya, H. Sugiyama, Y. Yamasaki, and H. Makino, "Transforming growth factor-β 1 induces vascular endothelial growth factor expression in murine proximal tubular epithelial cells," *Nephron Experimental Nephrology*, vol. 95, no. 2, pp. e79–86, 2003.

[21] P. Rosen, P. P. Nawroth, G. King, W. Moller, H. J. Tritschler, and L. Packer, "The role of oxidative stress in the onset and progression of diabetes and its complications: a summary of a congress series sponsored by UNESCO-MCBN, the American diabetes association and the German diabetes society," *Diabetes/Metabolism Research and Reviews*, vol. 17, no. 3, pp. 189–212, 2001.

[22] E. Herrera and C. Barbas, "Vitamin E: action, metabolism and perspectives," *Journal of Physiology and Biochemistry*, vol. 57, no. 2, pp. 43–56, 2001.

[23] M. G. Traber and J. Atkinson, "Vitamin E, antioxidant and nothing more," *Free Radical Biology and Medicine*, vol. 43, no. 1, pp. 4–15, 2007.

[24] D. M. Alscher, N. Braun, D. Biegger et al., "Induction of metallothionein in proximal tubular cells by zinc and its potential as an endogenous antioxidant," *Kidney and Blood Pressure Research*, vol. 28, no. 3, pp. 127–133, 2005.

[25] S. Zheng, E. C. Carlson, L. Yang, P. M. Kralik, Y. Huang, and P. N. Epstein, "Podocyte-specific overexpression of the antioxidant metallothionein reduces diabetic nephropathy," *Journal of the American Society of Nephrology*, vol. 19, no. 11, pp. 2077–2085, 2008.

Diabetologia
DOI 10.1007/s00125-010-2028-x

ARTICLE

Glucagon-like peptide-1 receptor agonist ameliorates renal injury through its anti-inflammatory action without lowering blood glucose level in a rat model of type 1 diabetes

R. Kodera · K. Shikata · H. U. Kataoka · T. Takatsuka · S. Miyamoto · M. Sasaki · N. Kajitani · S. Nishishita · K. Sarai · D. Hirota · C. Sato · D. Ogawa · H. Makino

Received: 4 June 2010 / Accepted: 30 November 2010

Abstract
Aims/hypothesis Glucagon-like peptide-1 (GLP-1) has various extra-pancreatic actions, in addition to its enhancement of insulin secretion from pancreatic beta cells. The GLP-1 receptor is produced in kidney tissue. However, the direct effect of GLP-1 on diabetic nephropathy remains unclear. Here we demonstrate that a GLP-1 receptor agonist, exendin-4, exerts renoprotective effects through its anti-inflammatory action via the GLP-1 receptor without lowering blood glucose.
Methods We administered exendin-4 at 10 μg/kg body weight daily for 8 weeks to a streptozotocin-induced rat model of type 1 diabetes and evaluated their urinary albumin excretion, metabolic data, histology and morphometry. We also examined the direct effects of exendin-4 on glomerular endothelial cells and macrophages in vitro.
Results Exendin-4 ameliorated albuminuria, glomerular hyperfiltration, glomerular hypertrophy and mesangial matrix expansion in the diabetic rats without changing blood pressure or body weight. Exendin-4 also prevented macrophage infiltration, and decreased protein levels of intercellular adhesion molecule-1 (ICAM-1) and type IV collagen, as well as decreasing oxidative stress and nuclear factor-κB activation in kidney tissue. In addition, we found that the GLP-1 receptor was produced on monocytes/macrophages and glomerular endothelial cells. We demonstrated that in vitro exendin-4 acted directly on the GLP-1 receptor, and attenuated release of pro-inflammatory cytokines from macrophages and ICAM-1 production on glomerular endothelial cells.
Conclusions/interpretation These results indicate that GLP-1 receptor agonists may prevent disease progression in the early stage of diabetic nephropathy through direct effects on the GLP-1 receptor in kidney tissue.

Keywords Anti-inflammatory effect · Diabetic nephropathy · Exendin-4 · Glomerular endothelial cells · GLP-1 receptor agonist · Intercellular adhesion molecule-1 · Macrophage · Nuclear factor-κB · Type 1 diabetic rats

Abbreviations

GLP-1	Glucagon-like peptide-1
GLP-1R	Glucagon-like peptide-1 receptor
hGECs	Human glomerular microvascular endothelial cells
ICAM-1	Intercellular adhesion molecule-1
NOX4	NADPH oxidase 4
NF-κB	Nuclear factor-κB
8-OHdG	8-Hydroxydeoxyguanosine

Electronic supplementary material The online version of this article (doi:10.1007/s00125-010-2028-x) contains supplementary material, which is available to authorised users.

R. Kodera · K. Shikata (✉) · H. U. Kataoka · T. Takatsuka · S. Miyamoto · M. Sasaki · N. Kajitani · S. Nishishita · K. Sarai · D. Hirota · C. Sato · H. Makino
Department of Medicine and Clinical Science,
Okayama University Graduate School of Medicine, Dentistry, and Pharmaceutical Sciences,
2-5-1 Shikata-cho,
Okayama 700-8558, Japan
e-mail: shikata@md.okayama-u.ac.jp

C. Sato · D. Ogawa
Department of Diabetic Nephropathy, Okayama University Graduate School of Medicine, Dentistry, and Pharmaceutical Sciences,
Okayama, Japan

Published online: 21 January 2011

Introduction

The number of patients with diabetes is increasing dramatically throughout the world, while diabetic nephropathy is the leading cause of end-stage renal disease in developed countries. In addition, chronic kidney disease contributes to development of cardiovascular disease and leads to an increase in all-cause mortality rates [1, 2]. Therefore, prevention of renal insufficiency improves the prognosis of diabetic patients.

Numerous factors contribute to the development of diabetic nephropathy, such as glomerular hyperfiltration [3], which is mainly observed in early-stage nephropathy, oxidative stress [4], accumulation of AGEs [5], activation of protein kinase C [6], acceleration of the polyol pathway and overexpression of TGF-β [7]. Accumulating evidence also points to the critical role of the inflammatory process in the development of diabetic vascular complications, suggesting that microinflammation is a common mechanism in pathogenesis of diabetic nephropathy [8, 9]. Furuta et al. [10] reported that infiltration of mononuclear cells was prominent in the glomeruli of patients with diabetic nephropathy. Our group has also reported similar results, as well as observing an increase in the production of cell adhesion molecules in the kidney of diabetic patients [11]. We found that intercellular adhesion molecule-1 (ICAM-1) played a key role in promoting macrophage infiltration in glomeruli from a rat model of diabetes [12], and using mice deficient in ICAM-1, we also showed that blockade of ICAM-1 activation ameliorated diabetic nephropathy [13]. Additionally, we showed that methotrexate, an immunosuppressant, ameliorated diabetic nephropathy and that anti-inflammatory agents also had a beneficial effect on diabetic nephropathy [14]. Modulation of the inflammatory process prevents renal injury in animal models of diabetes, suggesting that microinflammation is a potential therapeutic target in diabetic nephropathy [14–17].

Glucagon-like peptide-1 (GLP-1) is a gut incretin hormone and currently considered an attractive agent for treatment of type 2 diabetes. It has various beneficial effects on pancreatic beta cells, such as enhancement of glucose-dependent insulin secretion [18], acceleration of beta cell proliferation and inhibition of beta cell apoptosis [19]. In the gut and hypothalamus, GLP-1 inhibits motility, gastric emptying [20] and central regulation of feeding [21], resulting in body weight loss [18]. However, native GLP-1 is rapidly degraded in the circulation by dipeptidylpeptidase-IV [22]. Today, dipeptidylpeptidase-IV-resistant, long-acting GLP-1 receptor (GLP-1R) agonists such as exendin-4 and liraglutide are available for type 2 diabetic patients. Previous reports have shown that GLP-1R is produced not only in the pancreas, gut and hypothalamus, but also in the kidney [23–25]. With respect to the effects of GLP-1 on the kidney, it has been reported that exendin-4 ameliorated hypertension by regulating sodium excretion in tubular cells [26] and attenuated renal injury by improving metabolic anomalies in a mouse model of type 2 diabetes [25]. From these results, the amelioration of hypertension and metabolic anomalies by GLP-1 would seem to have a beneficial effect on diabetic nephropathy. In the present study, we focused on the direct effect of GLP-1 through GLP-1R in the kidney, independently of the numerous other effects of GLP-1, including its glucose-lowering action.

Methods

Animals

Male Sprague–Dawley rats (5 weeks old; Charles River, Yokohama, Japan) were divided into the following groups: (1) non-diabetes (n=5); (2) non-diabetes treated with exendin-4 (n=6); (3) diabetes (n=6); and (4) diabetes treated with exendin-4 (n=6). At the age of 5 weeks, the groups allocated to be made diabetic received intravenous injections of streptozotocin (Sigma-Aldrich, St Louis, MO, USA) at 65 mg/kg body weight in citrate buffer (pH 4.5). We included only rats with blood glucose concentrations >16 mmol/l at 3 and 7 days after streptozotocin injection in the diabetes groups. The non-diabetic groups received injections of citrate buffer alone. The two groups treated with exendin-4 were given exendin-4 (Bachem, Bubendorf, Switzerland) intraperitoneally at 10 μg/kg body weight daily for 8 weeks, starting at 1 week after the streptozotocin or citrate buffer injections. The placebo groups were given water alone using the same schedule as in the exendin-4 treatment groups. All rats had free access to standard chow and tap water. All procedures were performed according to the Guidelines for Animal Experiments at Okayama University Medical School, the Japanese Government Animal Protection and Management Law and the Japanese Government Notification on Feeding and Safekeeping of Animals. All rats were killed at 9 weeks after induction of diabetes in the diabetes groups, and the kidneys were weighed and fixed in 10% (vol./vol.) formalin, or frozen in acetone cooled on dry ice.

Metabolic variables

Systolic BP was measured by tail-cuff plethysmography (Softron, Tokyo, Japan). HbA_{1c} was measured by the HPLC method. Serum creatinine was measured by the 3-hydroxy-2,4,6-triiodobenzoic acid method. Food intake was calculat-

ed as the average over 3 days. Insulin concentration was measured by a rat insulin RIA kit (LincoResearch, St Charles, MO, USA). Urine samples were collected over a 24 h period in individual metabolism cages. Urinary albumin excretion was measured by nephelometry using anti-rat albumin antibody (ICN Pharmaceuticals, Aurora, OH, USA). Creatinine clearance (ml min^{-1} kg^{-1}) was calculated as described previously [15].

Light microscopy

The glomerular tuft area and mesangial matrix index (ratio of the mesangial matrix area/glomerular tuft area) were measured using a software package (Lumina Vision; Mitani, Fukui, Japan) as described previously [13]. Periodic acid–Schiff's reagent staining was used to observe the interstitium of the kidney. Quantitative analysis for all staining was performed in a blinded manner.

Immunoperoxidase staining

Immunoperoxidase staining was performed as described [12, 27]. Primary antibodies were macrophages mouse antibody (ED1, 1:50; Serotec, Oxford, UK), 8-hydroxydeoxyguanosin (8-OHdG) mouse antibody (1:10; JalCA, Shizuoka, Japan), NADPH oxidase 4 (NOX4) rabbit antibody (1:300; Novus Biologicals, Littleton, CO, USA) or GLP-1R rabbit antibody (ab39072, 1:200; Abcam, Tokyo, Japan), all of which were applied for 12 h at 4°C. Secondary antibodies were biotin-labelled anti-mouse or anti-rabbit IgG (Jackson ImmunoResearch, West Grove, PA, USA), which were applied for 60 min at room temperature. The average number of ED1-positive cells per glomerulus was used for the estimation. The ratio of the area stained positive with each of the above antibodies to the glomerular tuft area was calculated with a software package (Lumina Vision).

Immunofluorescence staining

Immunofluorescence staining was performed as described [12]. The primary antibodies were ICAM-1 mouse antibody (1:25; Abcam) or type IV collagen rabbit antibody (1:200; LSL, Tokyo, Japan), which were applied for 60 min at room temperature. Secondary antibodies were FITC-conjugated anti-mouse or anti-rabbit IgG (1:150; Zymed Laboratories, San Francisco, CA, USA), which were applied for 30 min at room temperature. Micrographic fluorescence photos were obtained with a laser-scanning confocal microscope (LSM-510; Carl Zeiss, Jena, Germany). The ICAM-1 and type IV collagen indexes were calculated as described [15].

Double immunofluorescence staining

The primary antibodies were GLP-1R rabbit antibody (1:200; Abcam) and rat endothelial cell antigen (RECA-1, 1:40; Monosan, Uden, the Netherlands), macrophages (ED1, 1:50) mouse antibody, or NOX4 rabbit antibody (1:300), which were applied for 12 h at 4°C. The secondary antibodies were Alexa-Fluor 488-labelled anti-rabbit and 546-labelled anti-mouse IgG (1:400; Invitrogen, Carlsbad, CA, USA), which were applied for 30 min at room temperature. Nuclei were stained with DAPI (Millipore, Tokyo, Japan). The sections were observed under a fluorescence microscope (BZ-800; Keyence, Osaka, Japan).

Quantitative real-time RT-PCR and gene expression

Total RNA was extracted from each sample (the rat renal cortex, glomeruli isolated by a previously reported mechanical sieving technique [28] and cultured cells) using a kit (RNeasy plus Mini; Qiagen, Valencia, CA, USA). Single-strand cDNA was synthesised from the individual samples of total RNA at 1 μg using a kit (GeneAmp RNA PCR-

Table 1 Metabolic variables of four rat groups at 8 weeks

Variable	Non-diabetic		Diabetic	
	Placebo	Exendin-4	Placebo	Exendin-4
Body weight (g)	471±23.5[a]	397±8.3[b]	256±30.5	246±22.9
Food intake (g/day)	27.6±0.9[c,d]	19.3±3.1[a]	44.6±12.5	38.6±0.5
HbA_{1c} (%)	3.7±0.1[a]	3.9±0.1[a]	10.5±0.5	10.0±0.8
Fasting blood glucose (mmol/l)	4.0±0.2[a]	4.9±0.3[a]	26.6±0.9	26.6±2.4
Systolic BP (mmHg)	115±2.6	114±1.5	120±1.3	123±2.6
Relative kidney weight (g/kg)	5.9±0.2[a]	6.1±0.1[a]	11.6±0.7	12.0±0.7

Values are the means ± SEM; $n=5$ animals in the non-diabetic placebo group; $n=6$ animals per group in the three other groups

[a] $p<0.001$ vs diabetes and diabetes + exendin-4 groups; [b] $p<0.01$ vs diabetes and diabetes + exendin-4 groups; [c] $p<0.001$ vs diabetes placebo group; [d] $p<0.05$ vs diabetes plus exendin-4 group

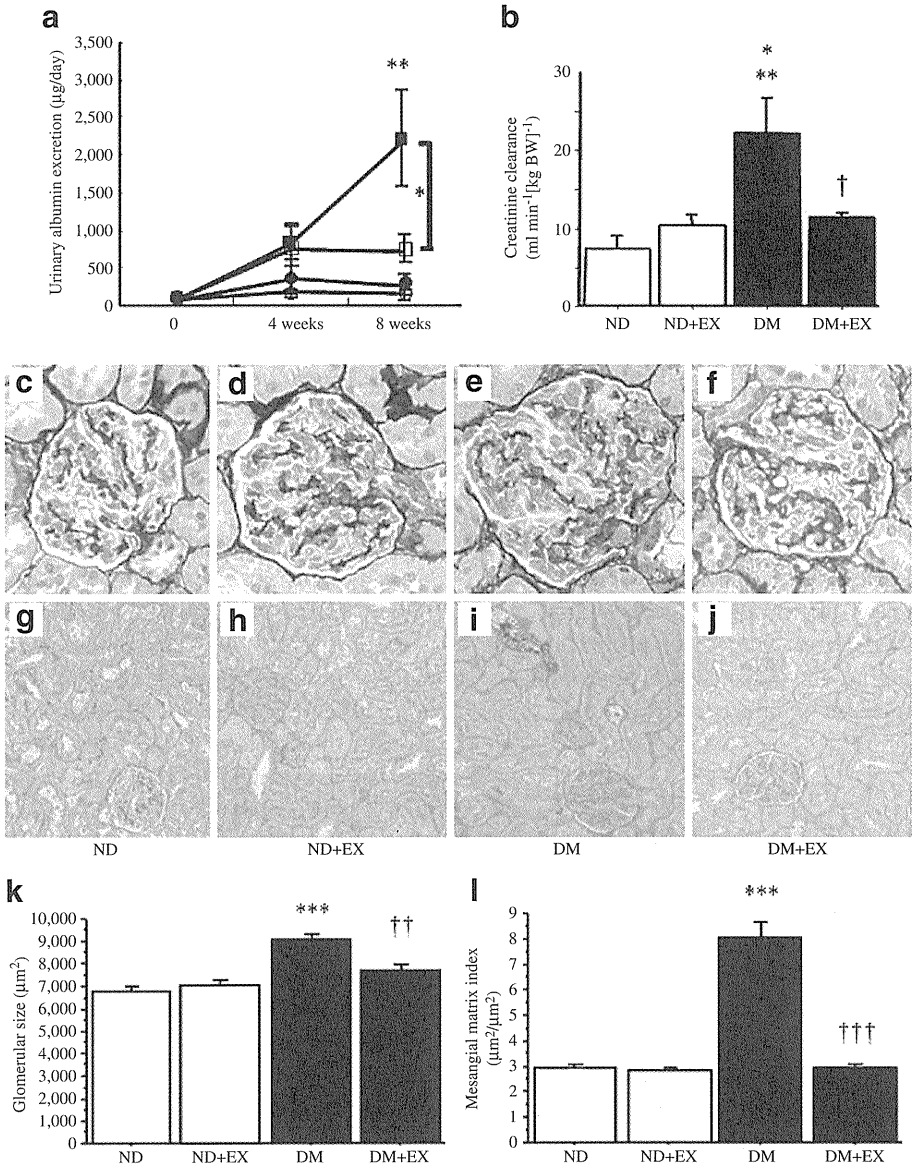

Fig. 1 **a** Time course of 24 h urinary albumin excretion. Urinary albumin excretion increased gradually over 8 weeks in the diabetic group. Exendin-4 resulted in a significantly lower level of urinary albumin excretion at 8 weeks than in the untreated diabetes group. *p <0.05; **p<0.01 vs non-diabetic and non-diabetic + exendin-4 groups. Black circles, non-diabetic group; white circles, non-diabetic + exendin-4; black squares, streptozotocin-induced diabetes group; white squares, diabetes + exendin-4 group. **b** Creatinine clearance. Hyperfiltration in the diabetic (DM) nephropathy group was significantly decreased by exendin-4 treatment (DM+EX) at 8 weeks. *p< 0.05 vs non-diabetic + exendin-4 (ND+EX); **p<0.01 vs ND; $^{\dagger}p$< 0.05 vs DM. **c–f** Periodic acid–methenamine-silver (PAM) staining in glomeruli (original magnification ×200). **g–j** Periodic acid–Schiff's reagent staining in the kidney (×100). **k** Glomerular size (tuft area). Glomerular hypertrophy was significantly greater in the DM group than in the ND groups. Exendin-4 treatment significantly suppressed glomerular hypertrophy. ***p<0.001 vs ND and ND+EX; $^{\dagger\dagger}p$<0.01 vs DM. **l** Mesangial matrix index, calculated by the PAM-positive area in the tuft area, was significantly increased in the DM group. Exendin-4 treatment significantly reduced mesangial matrix expansion. ***p< 0.001 vs ND and ND+EX; $^{\dagger\dagger\dagger}p$<0.001 vs DM. n=5 animals in the untreated ND group; n=6 animals per group in the three other groups. **k**, **l** Glomeruli: n=30 from each rat kidney; n=4 per group. Values are the means ± SEM

Core kit; Applied Biosystems, Foster City, CA, USA). After addition of each set of primers (final concentration 0.4 μmol/l) and template DNA to the master mix, quantitative real-time RT-PCR was performed with a LightCycler (Roche Diagnostics, Tokyo, Japan) and SYBR Premix-Ex-Taq (Takara Bio, Shiga, Japan). The PCR protocol was as follows: initial denaturation (95°C for 30 s), followed by 40 cycles of denaturation (95°C for 5 s), and annealing and extension (60°C for 20 s). The specific oligonucleotide primer sequences are shown in

Electronic supplementary material (ESM) Table 1. To visualise gene expression, individual DNA fragments were electrophoresed on a 2% (wt./vol) agarose gel (Sigma-Aldrich) and treated with ethidium bromide. cDNAs of the human pancreas (Takara Bio) and of rat islet-cell tumour cells (RIN-5F; DS Pharma Biomedical, Osaka, Japan) were used as positive controls.

Urinary 8-OHdG excretion

8-OHdG is a marker of oxidative DNA damage [29]. Urinary 8-OHdG concentration in a 24 h urine collection was measured with a kit (8-OHdG ELISA; JalCA) according to the manufacturer's instructions.

Nuclear factor-κB activation

Nuclear proteins of kidney tissues were extracted by a nuclear extract kit and nuclear factor-κB (NF-κB) p65 activity determined by ELISA using reagents (Active-Motif; Carlsbad, CA, USA) according to the manufacturer's instructions. Absorbance was normalised to milligram cell protein.

Western blotting

Cells were lysed with cell lysis buffer containing 10 mmol/l TRIS (pH 7.4), 1% (vol./vol.) Triton X-100, 0.5% (vol./vol.) Nonidet P-40 and phosphatase inhibitor cocktail, 150 mmol/l NaCl, 1 mmol/l EDTA, 0.2 mmol/l EGTA, vanadate and phenylmethanesulfonyl fluoride. The cell lysates were subjected to 7.5% SDS-PAGE (Bio-Rad Japan, Tokyo, Japan). The separated proteins were transferred to polyvinylidene fluoride membranes (Bio-Rad) by electrotransfer. The blots were subsequently blocked with 5% (vol./vol.) skimmed milk (Nacalai Tesque, Kyoto, Japan) and then incubated with GLP-1R rabbit antibody (1:500; Abcam) and ICAM-1 mouse antibody (1:100; Abcam) for 12 h at 4°C, or with β-actin rabbit antibody (1:1,000; Sigma-Aldrich) for 1 h at room temperature. The membrane was incubated with horseradish-peroxidase-linked donkey anti-rabbit or anti-mouse IgG (1:5,000; GE Healthcare Japan, Tokyo, Japan) at room temperature for 2 h. The blots were then visualised with a western blotting detection system (ECL plus; GE Healthcare).

Culture

Human glomerular microvascular endothelial cells (hGECs) (ACBRI, Kirkland, WA, USA) were cultured in EGM-MV2 medium (Cambrex, East Rutherford, NJ, USA) supplemented with 19.4 mmol/l D-glucose, 10% (vol./vol.) FCS and growth factor within a gelatin-precoated flask in a 5% CO_2 incubator at 37°C.

THP-1 cells (a human monocytic cell line; JCRB, Tokyo, Japan) were cultured in RPMI 1640 supplemented with 10 mmol/l D-glucose, 10% FCS and growth factor in a 5% CO_2 incubator at 37°C.

Human circulating monocytes

The human circulating monocytes were extracted using lymphocyte separation medium (MP Biomedicals, Tokyo, Japan) according to the manufacturer's instructions. After incubation in RPMI 1640 with 50 ng/ml phorbol myristate acetate (Sigma-Aldrich) for 24 h, total RNA was collected from the attaching cells as described above.

The effects of GLP-1 in THP-1 cells

THP-1 cells (1×10^6 cells/ml) were incubated for 24 h in six-well plates in RPMI 1640 medium supplemented with 1% FCS and 5.5 mmol/l D-glucose. THP-1 cells were exposed to the following conditions: (1) 5.5 mmol/l D-glucose (normal glucose); (2) 5.5 mmol/l D-glucose with 9.5 mmol/l mannitol (osmotic control); (3) 15 mmol/l D-glucose (high glucose); (4) high glucose with 2.5 nmol/l exendin-4; (5) high glucose with 10 nmol/l exendin-4; (6) high glucose with 100 nmol/l exendin-4; and (7) high glucose with 100 nmol/l exendin-4 and 1000 nmol/l GLP-1R antagonist (9-39) (Bachem). After incubation for 72 h, total RNA and supernatant fractions were collected from the cells. The supernatant fractions were measured using a human TNF-α and IL-1β immunoassay (Quantikine; R&D Systems, Minneapolis, MN, USA) according to the manufacturer's instructions.

The effect of GLP-1 in hGECs

After starvation for 12 h, hGECs were exposed to the following conditions: (1) no TNF-α stimulation (control); (2) 100 pg/ml TNF-α alone; (3) TNF-α with 2.5 nmol/l exendin-4; (4) TNF-α with 10 nmol/l exendin-4; (5) TNF-α with 100 nmol/l exendin-4; and (6) TNF-α with 100 nmol/l exendin-4 and 1000 nmol/l GLP-1R antagonist (9-39). After incubation for 6 h, total RNA and protein were collected from cells as described above. Recombinant human TNF-α was purchased from R&D Systems.

Statistical analysis

All values are expressed as the means ± SEM. Differences between groups were examined for statistical significance using the Mann–Whitney test or one-way ANOVA followed by Scheffe's test. Values of $p<0.05$ were considered to indicate statistically significant differences.

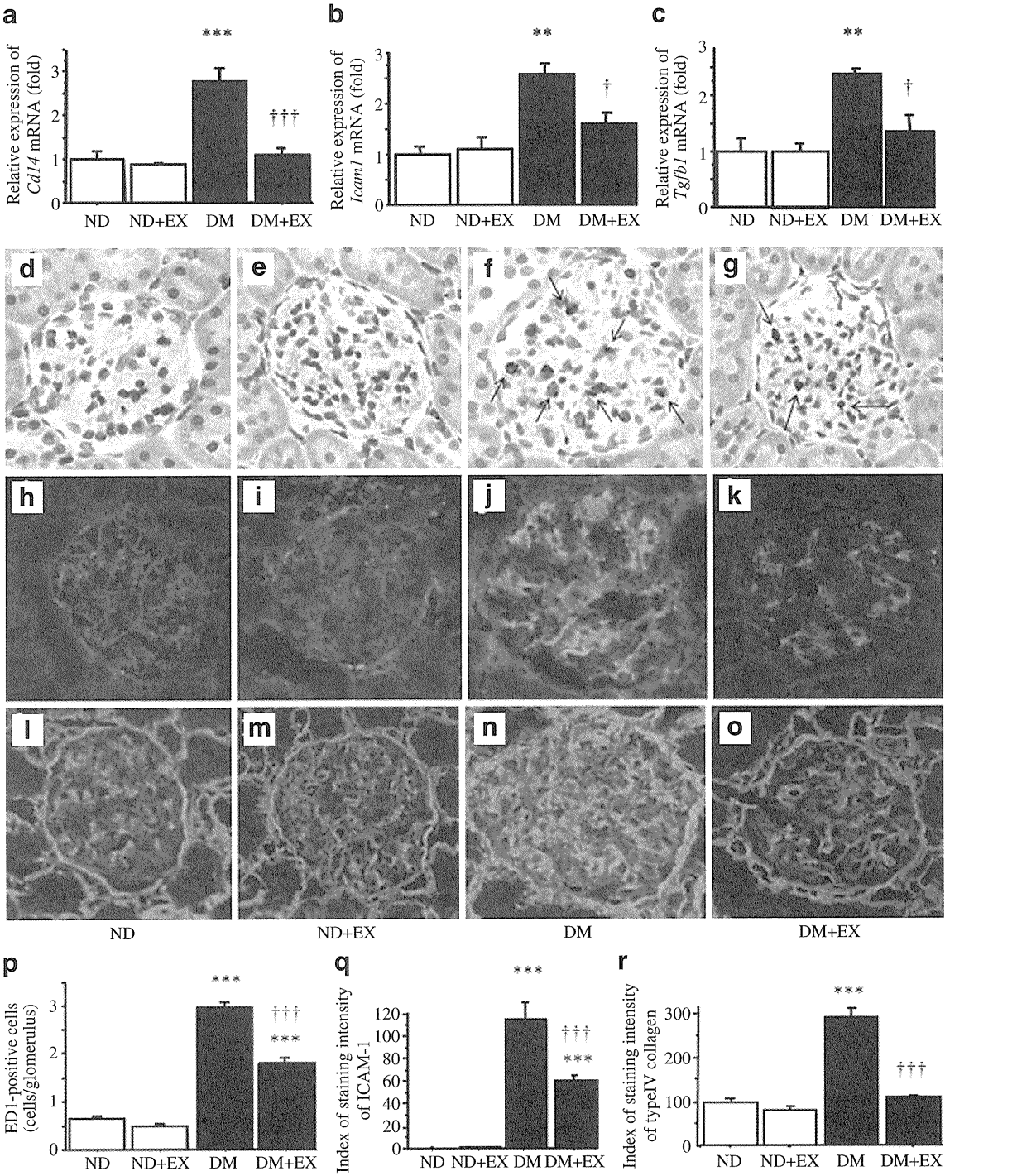

Fig. 2 Exendin-4 treatment suppressed the inflammatory axis in the kidney. **a** Quantification of *Cd14*, (**b**) *Icam1* and (**c**) *Tgfb1* gene expression by real-time RT-PCR in the renal cortex. All three genes were significantly downregulated by exendin-4 treatment. Values (means ± SEM) are presented as fold relative to *Actb* and expressed as 1 in ND; n=4 per group. Each experiment was performed three times. $^{**}p<0.01$ and $^{***}p<0.001$ vs non-diabetic (ND) and ND + exendin-4 (EX); $^{\dagger}p<0.05$ and $^{\dagger\dagger\dagger}p<0.001$ vs diabetes (DM). **d–g** Immunoperoxidase staining for macrophages (ED1-positive cells), indicated by arrows. **h–k** Immunofluorescence staining for ICAM-1 and (**l–o**) for type IV collagen. Magnification, all images ×200. **p** Quantification of the number of macrophages per glomerulus, which was significantly increased in the diabetic groups. Exendin-4 treatment significantly prevented glomerular macrophage infiltration in diabetes. $^{***}p<0.001$ vs ND and ND+EX; $^{\dagger\dagger\dagger}p<0.001$ vs DM. **q** Quantification of glomerular ICAM-1 staining per glomerulus, which was significantly increased in the diabetic groups and significantly reduced vs DM by exendin-4 treatment. $^{***}p<0.001$ vs ND and ND+EX; $^{\dagger\dagger\dagger}p<0.001$ vs DM. **r** Quantification of type IV collagen staining per glomerulus. Type IV collagen was significantly increased in the DM group and significantly reduced by exendin-4 treatment. $^{***}p<0.001$ vs ND and ND+EX; $^{\dagger\dagger\dagger}p<0.001$ vs DM. **p–r** Values are the means ± SEM; n=20 glomeruli from each rat kidney; n=4 per group. Each experiment was repeated three times

Results

Metabolic variables and urinary albumin excretion

Body, organ weights and systolic BP As seen in Table 1, body weights of the diabetic groups at 8 weeks after initiation of exendin-4 treatment were significantly lower than those of the non-diabetic groups. The kidney weights per body weight of the diabetic groups were significantly higher than those of the non-diabetic groups. There were no significant differences among the diabetic groups. Systolic BP was similar in all groups.

Food intake, HbA_{1c} and insulin Food intake and HbA_{1c} were significantly elevated in the diabetic groups. However, there were no significant differences among the diabetic groups. Although GLP-1 has beta cell-protective effects, serum insulin concentration was not detectable in the diabetic groups in spite of the high blood glucose levels (data not shown).

Urinary albumin excretion and creatinine clearance Urinary albumin excretion, which is a characteristic feature of the early stage of diabetic nephropathy, increased progressively in the diabetic groups during the study. Exendin-4 treatment significantly reduced urinary albumin excretion compared with that of the diabetes group at 8 weeks (Fig. 1a). In addition, exendin-4 treatment prevented diabetes-induced hyperfiltration (Fig. 1b).

Kidney morphology

The level of glomerular hypertrophy was significantly higher in the diabetes group than in non-diabetic groups. In contrast, exendin-4 treatment inhibited glomerular hypertrophy (Fig. 1c–f, k) in diabetes. Quantitative analysis showed that mesangial matrix index, which was used as an index of mesangial expansion, was significantly increased in the diabetes group. However, exendin-4 treatment significantly reduced mesangial matrix expansion (Fig. 1l). The renal interstitium showed a significantly higher level of tubular hypertrophy in the diabetic groups than in non-diabetic groups. However, there was no remarkable difference among the diabetic groups. In addition, no histological change of fibrosis in the renal interstitium was seen in any of the groups (Fig. 1g–j).

Microinflammation in the kidney

To evaluate the anti-inflammatory effect of exendin-4 in the kidney, we examined gene expression of *Cd14*, which is regarded as a cell surface marker of macrophages, as well as expression of *Icam1* and *Tgfb1* in the cortex. *Cd14*, *Icam1* and *Tgfb1* were significantly upregulated in the diabetes group and significantly downregulated by exendin-4 treatment (Fig. 2a–c). Regarding the glomeruli, we evaluated macrophage infiltration, and ICAM-1 and type IV collagen levels in glomeruli. The number of macrophages in glomeruli was significantly elevated in the diabetic compared with the non-diabetic groups. In contrast, exendin-4 treatment significantly prevented glomerular macrophage infiltration (Fig. 2d–g, p) in diabetes. The ICAM-1 level was significantly increased in the diabetic groups, but was significantly reduced by exendin-4 treatment (Fig. 2h–k, q). The type IV collagen level, which is an important component in the mesangial matrix, was significantly increased in the diabetes group and significantly reduced by exendin-4 treatment (Fig. 2l–o, r).

Influence of exendin-4 on oxidative stress

To evaluate oxidative stress, we focused on 8-OHdG and NOX4. Urinary excretion of 8-OHdG was significantly increased in the diabetic groups compared with the non-diabetic groups. Exendin-4 treatment significantly decreased urinary excretion of 8-OHdG in diabetes (Fig. 3a). Immunoperoxidase staining for 8-OHdG revealed a significant abundance of 8-OHdG in glomeruli in the diabetic groups, which was significantly reduced by exendin-4 treatment (Fig. 3b–e, j). *Nox4* gene expression in the cortex was significantly upregulated in the diabetes group and significantly downregulated by exendin-4 treatment (Fig. 3k). We demonstrated the presence of NOX4 in glomerular endothelial cells in the rat kidney (ESM Fig. 1h–k). Immunoperoxidase staining for NOX4 revealed a significant abundance of NOX4 in the diabetic kidney. However, exendin-4 treatment significantly reduced the level of NOX4 in diabetes (Fig. 3f–i, l).

NF-κB activation in the kidney

The activation of NF-κB p65 DNA-binding activity was significantly enhanced in the diabetes compared with the non-diabetic groups. Exendin-4 treatment significantly inhibited NF-κB p65 DNA-binding activity in diabetes (Fig. 3m).

GLP-1R in rat glomeruli

We demonstrated the existence of GLP-1R in rat glomeruli (Fig. 4a, d). Double immunofluorescence staining revealed production of GLP-1R on glomerular endothelial cells (Fig. 4e–h). In addition, we ascertained that GLP-1R was produced on macrophages in rat glomeruli (Fig. 4i–l). The GLP-1R levels in glomeruli were not significantly different among the groups (ESM Fig. 1a–g).

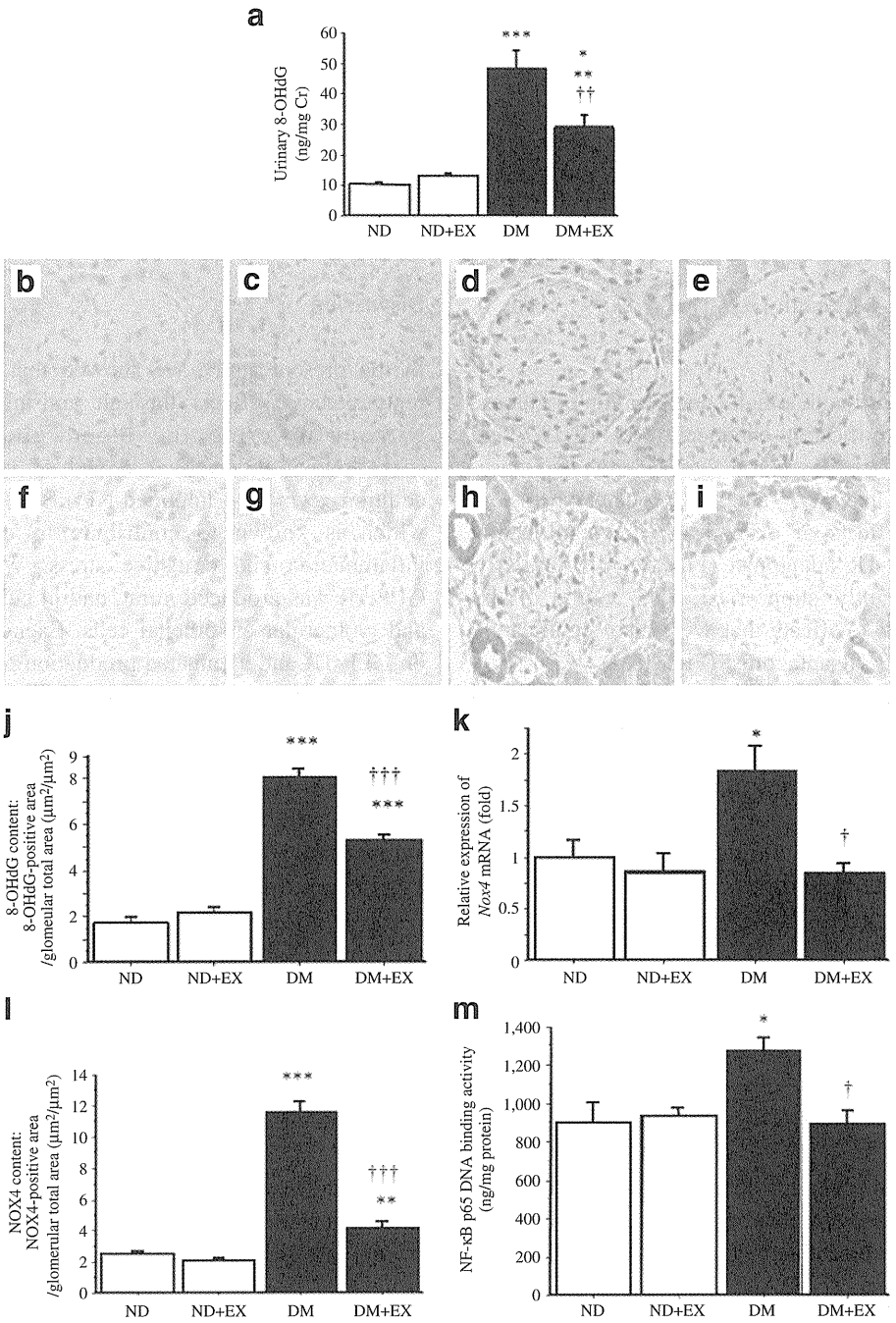

Fig. 3 Exendin-4 treatment suppressed oxidative stress and NF-κB activation. **a** Urinary 8-OHdG concentration in a 24 h urine collection. Urinary 8-OHdG excretion was significantly increased in the diabetic groups (DM). However, exendin-4 treatment (EX) significantly decreased urinary 8-OHdG excretion; n=5 per group. The experiment was repeated twice. *p<0.05 vs non-diabetic (ND)+EX; **p<0.01 vs ND; ***p<0.001 vs ND and ND+EX; $^{\dagger\dagger}p$<0.01 vs DM. **b–e** Immunoperoxidase staining for 8-OHdG and (**f–i**) NOX4 in glomeruli. Magnification, all images ×200. **j** Quantification of 8-OHdG content (μm²/μm²) as staining per glomerulus. Glomerular 8-OHdG content was significantly increased in the diabetic groups and significantly reduced by exendin-4 treatment. Values are means ± SEM; n=20 glomeruli from each rat kidney; n=4 per group. ***p<0.001 vs ND and ND+EX; $^{\dagger\dagger\dagger}p$ <0.001 vs DM. **k** Quantification of *Nox4* by real-time RT-PCR in the renal cortex. *Nox4* expression was significantly downregulated by exendin-4 treatment. Values (means ± SEM) are presented as fold relative to *Actb* and expressed as 1 in ND; n=4 per group. Each experiment was repeated three times. *p<0.05 vs ND and ND+EX; $^{\dagger}p$< 0.05 vs DM. **l** Quantification of NOX4 content (μm²/μm²) as staining per glomerulus. NOX4 content was significantly increased in the diabetic groups and significantly suppressed by exendin-4 treatment. Values are means ± SEM; n=20 glomeruli from each rat kidney; n=4 per group. **p<0.01 and ***p<0.001 vs ND and ND+EX; $^{\dagger\dagger\dagger}p$<0.001 vs DM. **m** NF-kB p65 DNA-binding activity. NF-κB p65DNA-binding activity was significantly increased in the DM group. Exendin-4 treatment significantly decreased NF-κB p65 DNA-binding activity. Values are the means ± SEM; n=5 per group. The experiment was repeated twice. *p<0.05 vs ND and ND+EX; $^{\dagger}p$<0.05 vs DM

GLP-1R in human macrophages and hGECs

We identified the existence of GLP-1R in THP-1 cells and hGECs (Figs 5a, b and 6a, b). In addition, we examined *GLP1R* gene expression in human circulating monocytes. We demonstrated that the *GLP-1R* gene was not only expressed in the THP-1 cell line, but also in human circulating monocytes (Fig. 5a).

The effects of GLP-1 through GLP-1R on THP-1 cells and hGECs

THP-1 cells stimulated with a high concentration of glucose for 72 h showed significantly enhanced levels of *TNF* and *IL1B* gene expression. Exendin-4 significantly and dose-dependently attenuated *TNF* and *IL1B* gene expression. Additionally, the effects of exendin-4 were significantly blocked by a GLP-1R antagonist (Fig. 5c, d). Similarly, exendin-4 significantly suppressed TNF-α and IL-1β secretion from THP-1, effects that were also significantly blocked by the GLP-1R antagonist (Fig. 5e, f).

hGECs stimulated with TNF-α for 6 h showed significantly enhanced *ICAM1* gene expression. Exendin-4 significantly and dose-dependently attenuated *ICAM1* gene expression. In addition, the effect of exendin-4 was significantly blocked by the GLP-1R antagonist (Fig. 6c). Likewise, exendin-4 significantly suppressed TNF-α-induced ICAM-1 production on hGECs, an effect that, again, was also significantly blocked by the GLP-1R antagonist (Fig. 6d, e).

Discussion

In the present study, we showed that exendin-4 exerted renoprotective effects through anti-inflammatory actions without lowering the blood glucose level in a streptozotocin-induced rat model of type 1 diabetes. In addition, exendin-4 inhibited NF-κB activity in the kidney, which is known to contribute to cross-talk between inflammation and oxidative stress. We also found that GLP-1R was produced in rat, and in cultured macrophages and glomerular endothelial cells. Exendin-4 acted directly on GLP-1R and attenuated production of pro-inflammatory cytokines and ICAM-1 in vitro. This is the first report of a GLP-1R agonist directly contributing, via its anti-

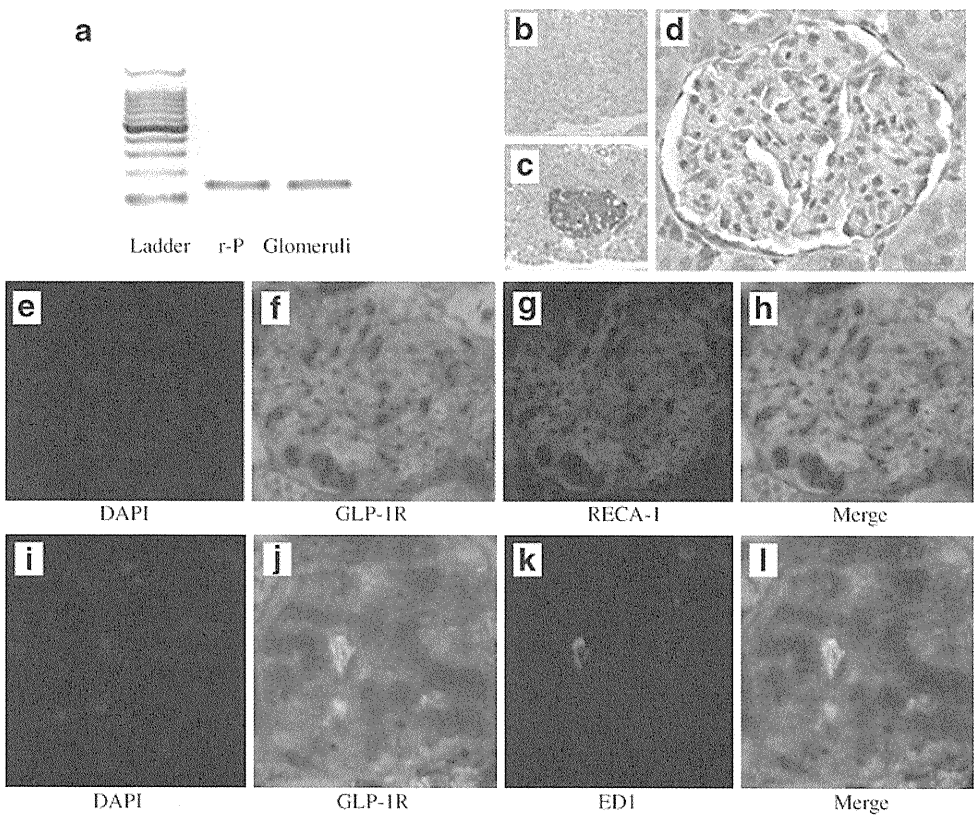

Fig. 4 The production of GLP-1R in rat glomeruli. **a** *Glp1r* gene expression in rat glomeruli. r-P: rat positive control (RIN-5F: rat islet-cell tumour). **b** Immunoperoxidase staining for GLP-1R, with negative control in rat pancreas islet cells, (**c**) positive control in rat pancreas islet cells and (**d**) rat glomeruli. **e–h** Double immunofluorescence staining for GLP-1R and glomerular endothelial cells as labelled. RECA-1, rat endothelial cell antigen. **i–l** Double immunofluorescence staining for GLP-1R and macrophages

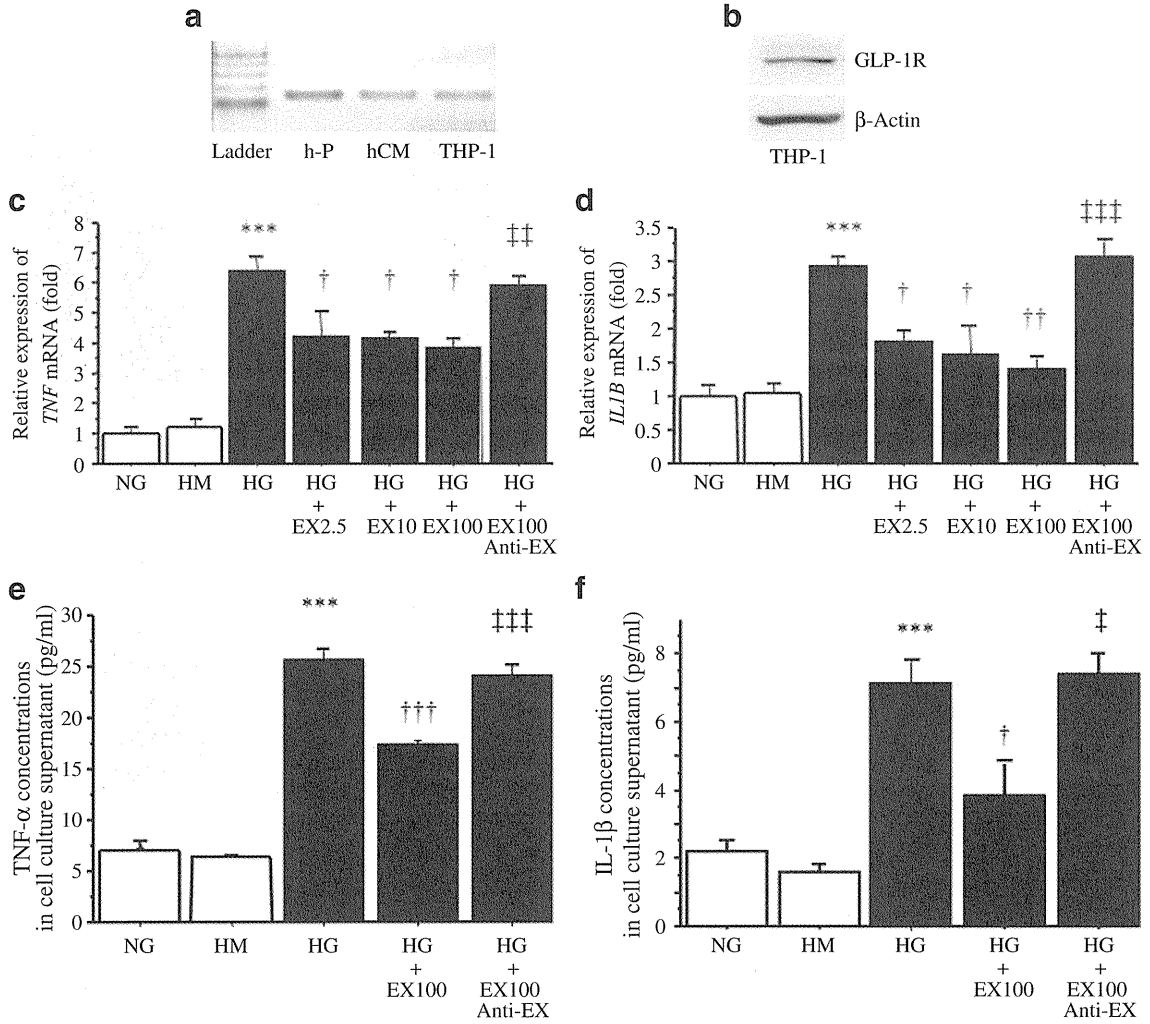

Fig. 5 The direct effects of exendin-4 on THP-1 cells. **a** *GLP1R* gene expression in human circulating monocytes (hCM) and THP-1 cells. h-P, human positive control (human pancreas). **b** GLP-1R protein production in THP-1 cells by western blotting. **c** Quantification of *TNF* and (**d**) *IL1B* mRNA expression in THP-1 by real-time RT-PCR. THP-1 cells stimulated with 15 mmol/l high glucose (HG; 15.0 mmol/l D-glucose) for 72 h showed significantly enhanced *TNF* and *IL1B* expression. Exendin-4 (EX) significantly and dose-dependently suppressed *TNF* and *IL1B* gene expression. GLP-1R antagonist (anti-EX; 1,000 nmol/l) significantly inhibited the suppressive effects of exendin-4 (100 nmol/l) on *TNF* and *IL1B* expression. Values (means ± SEM) are presented as fold relative to *GAPDH* and expressed as 1 in normal glucose (NG; 5.5 mmol/l D-glucose), n=5 per group. The experiment was repeated three times. ***$p<0.001$ vs NG and 5.5 mmol/l D-glucose with 9.5 mmol/l mannitol (HM); $^{\dagger}p<0.05$ and $^{\dagger\dagger}p<0.01$ vs HG; $^{\ddagger\ddagger}p<0.01$ and $^{\ddagger\ddagger\ddagger}p<0.001$ vs HG+EX (100 nmol/l; EX100). **e** Quantification of TNF-α and (**f**) IL-1β secretion (pg/ml) from THP-1 by ELISA. Stimulation of THP-1 cells with HG for 72 h significantly promoted TNF-α and IL-1β secretion. Exendin-4 significantly suppressed TNF-α and IL-1β secretion. GLP-1R antagonist (anti-EX; 1,000 nmol/l) significantly inhibited the suppressive effects of exendin-4 (100 nmol/l) on TNF-α and IL-1β secretion. Values are the means ± SEM; n=5 per group. The experiment was repeated twice. ***$p<0.001$ vs NG and HM; $^{\dagger}p<0.05$ and $^{\dagger\dagger\dagger}p<0.001$ vs HG; $^{\ddagger}p<0.05$ and $^{\ddagger\ddagger\ddagger}p<0.001$ vs HG+EX100. EX2.5, 2.5 nmol/l exendin-4; EX10, 10 nmol/l exendin-4

inflammatory effects, to amelioration of characteristic features of diabetic nephropathy, such as increased urinary albumin excretion, glomerular hypertrophy and mesangial matrix expansion.

The current results suggest that exendin-4 alleviated the above-mentioned features by suppressing: (1) ICAM-1 production; (2) macrophage infiltration; (3) NF-κB activation; (4) oxidative stress; and (5) *Tgfb1* mRNA expression and type IV collagen accumulation in the kidney.

An increase in the level of ICAM-1 on glomerular endothelial cells promotes macrophage infiltration into glomeruli [12, 14]. In our study, exendin-4 prevented macrophage infiltration into glomeruli. The mechanism underlying this effect was thought to be the suppression of ICAM-1 production on glomerular endothelial cells and direct inhibition of cytokine release from macrophages, which breaks the vicious cycle between macrophages and glomerular endothelial cells that gives rise to microinflam-